Order Number 1333595

A theoretical study of nonlinear guided waves

Gubbels, Monica Ann, M.S.

The University of Arizona, 1988

U·M·I
300 N. Zeeb Rd.
Ann Arbor, MI 48106

PLEASE NOTE:

In all cases this material has been filmed in the best possible way from the available copy. Problems encountered with this document have been identified here with a check mark __✓__.

1. Glossy photographs or pages _____
2. Colored illustrations, paper or print _____
3. Photographs with dark background _____
4. Illustrations are poor copy _____
5. Pages with black marks, not original copy __✓__
6. Print shows through as there is text on both sides of page _____
7. Indistinct, broken or small print on several pages _____
8. Print exceeds margin requirements _____
9. Tightly bound copy with print lost in spine _____
10. Computer printout pages with indistinct print _____
11. Page(s) _____ lacking when material received, and not available from school or author.
12. Page(s) _____ seem to be missing in numbering only as text follows.
13. Two pages numbered _____. Text follows.
14. Curling and wrinkled pages _____
15. Dissertation contains pages with print at a slant, filmed as received _____
16. Other _____

_____

_____

A THEORETICAL STUDY OF NONLINEAR GUIDED WAVES

by

Monica Ann Gubbels

A Thesis Submitted to the Faculty of the

COMMITTEE ON OPTICAL SCIENCES (GRADUATE)

In Partial Fulfillment of the Requirements

For the Degree of

MASTER OF SCIENCE

In the Graduate College

THE UNIVERSITY OF ARIZONA

1 9 8 8

STATEMENT BY AUTHOR

This thesis has been submitted in partial fulfillment of requirements for an advanced degree at The University of Arizona and is deposited in the University Library to be made available to borrowers under rules of the Library.

Brief quotations from this thesis are allowable without special permission, provided that accurate acknowledgment of source is made. Requests for permission for extended quotation from or reproduction of this manuscript in whole or in part may be granted by the head of the major department or the Dean of the Graduate College when in his or her judgement the proposed use of the material is in the interests of scholarship. In all other instances, however, permission must be obtained from the author.

SIGNED: Monica A Stubbels

APPROVAL BY THESIS DIRECTOR

This thesis has been approved on the date shown below:

M. A. Stegeman — April 12, 1988

Dr. George Stegeman
Professor of Optical Sciences

Date

ACKNOWLEDGEMENTS

This work was made possible by several people, principally Dr. George Stegeman, without whom there would have been no work, and Dr. Ewan Wright, without whom the work would have been no fun. I offer special thanks to Ewan Wright for his guidance and insightfulness throughout the project. I also extend thanks to Dr. Jerry Moloney, Dr. Colin Seaton and the rest of Dr. Stegeman's group whose encouragement and discussion were invaluable, and thanks to Pat Gransie for her generous assistance.

Finally, I owe very special thanks to Merrick Firestone for his encouragement, patience and compassion throughout these school years.

TABLE OF CONTENTS

LIST OF ILLUSTRATIONS

ABSTRACT

The effect of linear absorption on TE_0 nonlinear guided waves and the effect of linear absorption, input-beam misalignment and nonlinear saturation on soliton emission from a nonlinear waveguide have been numerically investigated using the beam propagation method. In the first case the distribution of the absorption is found to have a dramatic effect on the propagation of the nonlinear guided waves. In the second case results reminiscent of the lossless case are found to survive in the presence of these complications.

I INTRODUCTION

The phenomenon of light waves guided by thin dielectric films bounded by media of less refractive index has been theoretically studied and observed experimentally [1, 2]. Generally these waveguides, often called planar or slab waveguides, consist of three layered media, with the outer two much thicker than the inner film. The first studies assumed that the refractive indices of these media were independent of the local field intensity. Such waveguides can be considered linear waveguides. Later dielectric media whose refractive index depends on the local field intensity were introduced into these studies [3-14]. A waveguide containing one or more of this type of media is called a nonlinear waveguide. An exciting aspect of nonlinear waveguides is that the properties of guided waves, i.e. the field profiles and effective indices, can become flux dependent. Nonlinear waveguides have received a great deal of attention as they display many interesting characteristics.

By assuming a lossless structure exact solutions to the nonlinear wave equation for transverse electric (TE) waves can be found for a nonlinear waveguide displaying a Kerr-type nonlinearity [15, 16]. For media of the Kerr-type the refractive index is proportional to the local field intensity. Using a formalism developed by Langbein et. al. [20, 21] and applied by Stegeman et. al. [22, 23] it is possible to deal with arbitrary local nonlinearities for the lossless case. From this formalism a dispersion curve between the guided wave flux S and the effective index β can be found [4]. An intriguing phenomenon occurs when in some cases the dispersion curve becomes highly distorted such that more than one guided wave solution, or corresponding β value, is possible for a given flux. Furthermore, on

some curves there is a maximum flux value above which a guided wave cannot exist. These features of the distorted dispersion curve suggest applications in nonlinear coupling and optical limiting.

From the formalism mentioned above we can choose a flux and effective index combination that lies on the dispersion curve and construct the transverse field profile of the corresponding nonlinear guided wave, a nonlinear guided wave being a wave which propagates down the guide unchanged in amplitude and phase in the transverse direction. The propagation of nonlinear guided waves is an important factor neglected in the early studies. Several nonlinear optical devices were proposed on the basis of the dispersion curves alone [24]. Using the beam propagation method [25], Moloney et. al. [26] studied the stability of the nonlinear guided waves under propagation. With the same method Wright et. al. [27] showed that a nonlinear guided wave can be excited using an appropriately chosen Gaussian beam. The propagation characteristics of nonlinear waveguides are of particular interest for applications to real devices.

In the ideal case a nonlinear guided wave propagates unchanged down the guide. One of the requirements for the ideal case is that the system be lossless. However, it is of interest to know what happens to the beam profile under propagation when the system is not lossless, in the presence of absorption. In this thesis we look at the effect of absorption on TE_0 nonlinear guided wave excitation and propagation.

It is necessary to test the stability of these guided wave solutions under propagation and, indeed, they have been tested using numerical techniques [26, 28, 29]. During the earlier work on stability of the nonlinear guided waves an interesting phenomena was noted for some of the unstable waves. As expected, some

of these waves displayed their instability by oscillating back and forth in the guide, however in other cases a portion of the beam actually broke off into the bounding media and propagated away from the guide. These solitary wave-packets are solitons and possess a property such that two identical waves traveling at a slight angle to each other pass through each other with only a change in phase. This soliton emission phenomenon attracted new research interest and many studies have been performed solely on these solitons. These solitons propagate unchanged under ideal conditions but what happens to them in nonperfect conditions? The latter part of this thesis discusses the effect that input beam misalignment, absorption and saturation have on this soliton emission.

In the next section we first derive the nonlinear wave equation that applies to our waveguide. Secondly, we discuss the waveguide used and the resulting nonlinear guided waves and dispersion curves. We also look at the previous work on the stability of these waves and their excitation by Gaussian beams. The third section contains the analysis of the effects of absorption on the propagation and excitation of nonlinear guided waves; while the fourth one the effects of nonideal conditions on soliton emission. The final section of this thesis contains a brief summary of the research and a few conclusions made from the results.

II TRANSVERSE ELECTRIC WAVE EQUATION AND GUIDED WAVES

II.1 General Transverse Electric Wave Equation

We begin our treatment of guided waves by discussing the properties of electromagnetic waves. The fields of any electromagnetic wave must satisfy Maxwell's equations which are [1, 2]

$$\nabla \cdot \mathbf{D} = 0 , \tag{2.1}$$

$$\nabla \cdot \mathbf{B} = 0 , \tag{2.2}$$

$$\nabla \times \mathbf{E} = -\frac{\partial \mathbf{B}}{\partial t} , \tag{2.3}$$

$$\nabla \times \mathbf{H} = \frac{\partial \mathbf{D}}{\partial t} , \tag{2.4}$$

in the absence of free current or charge density, where $\mathbf{B} = \mu_0 \mathbf{H}$ for a nonmagnetic medium. If we take the curl of Eq. 2.3 and employ 2.4 we find:

$$\nabla \times (\nabla \times \mathbf{E}) = \nabla (\nabla \cdot \mathbf{E}) - \nabla^2 \mathbf{E} = - \mu_0 \frac{\partial^2 \mathbf{D}}{\partial t^2}. \tag{2.5}$$

We consider an isotropic medium thus the displacement vector is given by $\mathbf{D} = \epsilon_0 n^2(r) \mathbf{E}$, where n(r) is the refractive index distribution of the medium and ϵ_0 is the permitivity of free space. In addition, we choose z to be the direction of propagation and the medium to be homogeneous in the y direction so that n(r) = n(x,z). We restrict our discussion to monochromatic transverse electric (TE) waves of frequency ω, the electric field can then be written [1, 2]

$$E(r,t) = \frac{1}{2}\, j\, (E(x,z)e^{-i\omega t} + c.c.) \tag{2.6}$$

where j is the unit vector in the y direction. Transverse magnetic waves could also be studied, however their analysis is more complicated than necessary for our purposes. The simplicity of TE waves will become apparent shortly. From the form of the solution in Eq. 2.6 we see that $\nabla \cdot E = 0$. This greatly simplifies Eq. 2.5 as now we can rewrite this equation solely in terms of E,

$$\nabla^2 E - \epsilon_0 n^2(r)\mu_0 \frac{\partial^2 E}{\partial t^2} = 0. \tag{2.7}$$

If we substitute our solution Eq. 2.6 into Eq. 2.7, it can be simplified to give:

$$\nabla^2 E(x,z) + k_0^2 n^2(x,z)E(x,z) = 0 \tag{2.8}$$

where $k_0^2 = \omega^2\mu_0\epsilon_0$ is the square of the free-space wavenumber. For a wave propagating predominantly in the z direction with a mean effective index β we can write

$$E(x,z) = \mathcal{E}(x,z)e^{i\beta k_0 z}. \tag{2.9}$$

By expanding the Laplacian in equation 2.8 and using 2.9 we obtain

$$\frac{\partial^2}{\partial x^2}\mathcal{E}(x,z) + 2ik_0\beta \frac{\partial \mathcal{E}(x,z)}{\partial z} + k_0^2(n^2(x,z) - \beta^2)\mathcal{E}(x,z) = 0\ . \tag{2.10}$$

Here we have used the slowly varying envelope approximation, that is the electric

field envelope $\mathcal{E}(x,z)$ varies slowly with respect to the plane-wave exponential factor, $|\partial^2\mathcal{E}/\partial z^2| \ll |\partial\mathcal{E}/\partial z|\beta k_0 \ll |\mathcal{E}|\beta^2 k_0^2$. In this approximation we neglect $|\partial^2\mathcal{E}/\partial z^2|$. Equation 2.10 is the basic wave equation for studying TE waves in waveguides.

II.2 Linear Guided Waves

In general a planar or slab waveguide consists of three homogeneous media. One medium is a thin film we choose to have a thickness 2d and to be unbounded in the y direction. The other two media bound this film on either side with the interfaces perpendicular to the x axis. These two media bounding the film are referred to as the cladding and substrate. Figure 2.1 displays this basic configuration with the coordinate system chosen. Recall that previously we chose z to be the propagation direction of the light.

In the linear case the refractive index distribution n(r) is independent of the field intensity and is solely dependent on the transverse coordinate x perpendicular to the direction of propagation, $n(r) = n(x)$. The linear guided wave solutions are easily found. They must satisfy the boundary conditions that the tangential components of the electric and magnetic vector fields be continuous across any interface. As we have chosen TE waves it can be shown that the continuity condition of the magnetic field is synonymous with requiring the continuity of the derivative of the electric field with respect to the transverse (x) axis. We see from the form of our electric field, Eq. 2.9, that our condition that E and $\partial E/\partial x$ are continuous requires $\mathcal{E}$ and $\partial\mathcal{E}/\partial x$ be continuous across the interfaces. For a stationary wave $\mathcal{E}(x,z)$ is independent of z, $\mathcal{E}(x,z) = \mathcal{E}(x)$, and our wave equation becomes

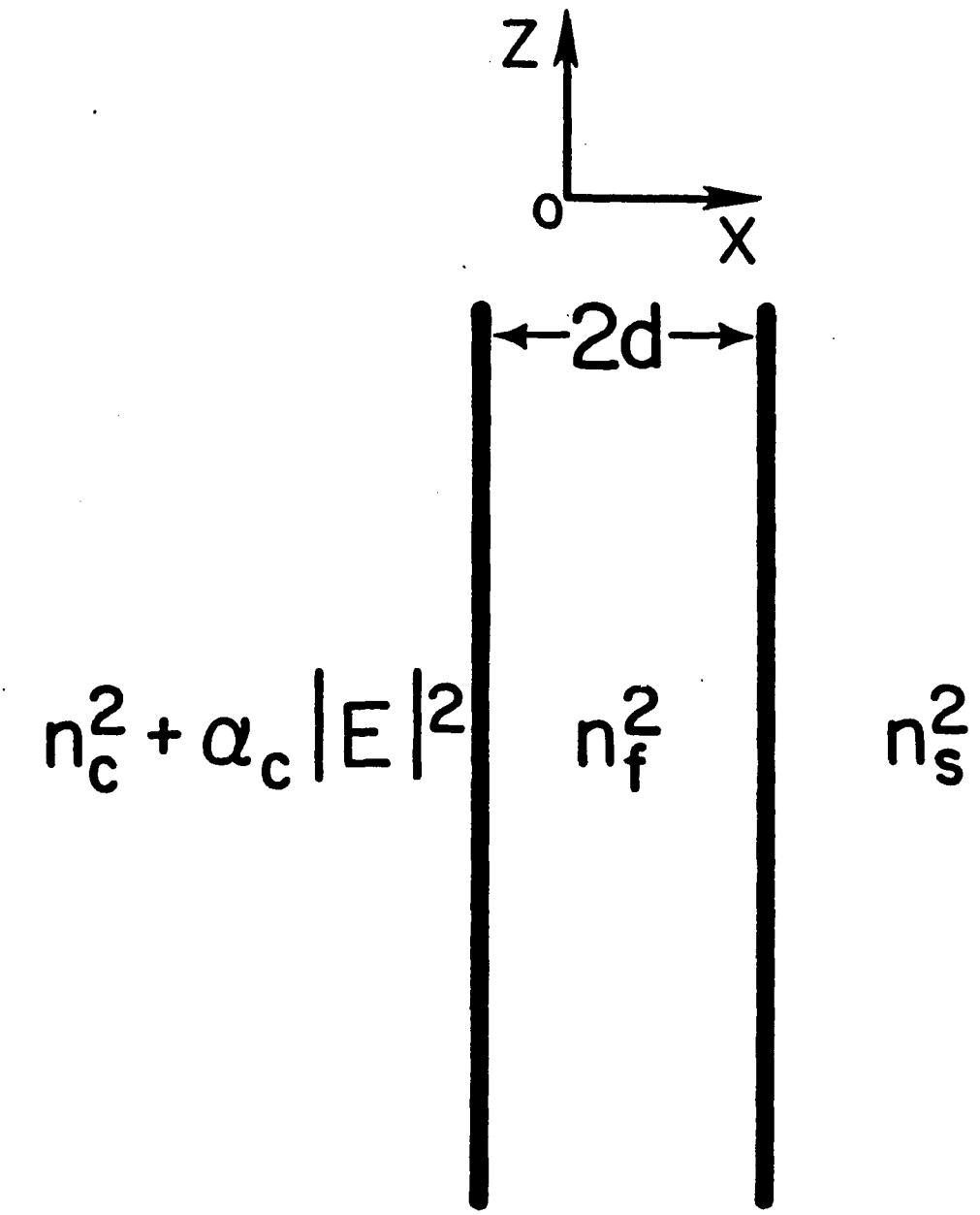

Fig. 2.1. Nonlinear waveguide geometry, a linear thin film of thickness 2d, bounded by a linear substrate and a nonlinear cladding.

$$\frac{d^2}{dx^2}\mathcal{E}_i(x) + k_0^2(n_i^2 - \beta^2)\mathcal{E}_i(x) = 0 \qquad (2.11)$$

where i = 1, 2, 3 stands for the cladding, film and substrate, respectively. Given a film of thickness of 2d with interfaces at x = +d and x = -d we can impose the above boundary conditions along with the condition that the electric field must decay to zero as x goes to $\pm\infty$ for physical solutions. A guided mode is a solution of the wave equation 2.11 that propagates down the guide unchanged in amplitude and phase if we assume ideal conditions. A solution that satisfies these boundary conditions requires that $n_2 > \beta > \max(n_1, n_3)$, the fields in regions 1 and 3 be exponential, and that in region 2 should be sinusoidal [1, 2]. It has the form:

$$\mathcal{E}_1(x) = \exp\{ (x + d)k_0 q_1 \} \qquad (2.12)$$

$$\mathcal{E}_2(x) = \cos[(x + d)k_0q_2] + A \sin[(x + d) k_0q_2] \qquad (2.13)$$

$$\mathcal{E}_3(x) = (\cos[2dk_0q_2] + A \sin[2dk_0q_2])\exp\{ -(x - d)k_0q_3 \} \qquad (2.14)$$

where $q_i^2 = |\beta^2 - n_i^2|$ and $A = q_1/q_2$. Note that this form of the solution ensures that $\mathcal{E}(x)$ is continuous. This is the basic solution to the linear, stationary, TE wave equation. From these three equations we can obtain relationships between various parameters that give us information about linear waveguides. One relation of interest is that between the product $2dk_0$ and the effective index β. By equating the transverse derivative of the electric field across the x = +d boundary (i.e. the film-substrate boundary) we obtain the relationship:

$$\tan(2k_0dq_2) = \left[1 + \frac{q_1}{q_3}\right] / \left[\frac{q_2}{q_3} - \frac{q_1}{q_2}\right] . \qquad (2.15)$$

We can solve this equation for the product $2k_0d$ in terms of the effective index β. A plot of this relation for both the TE_0 and TE_1 solutions appears in figure 2.2, where

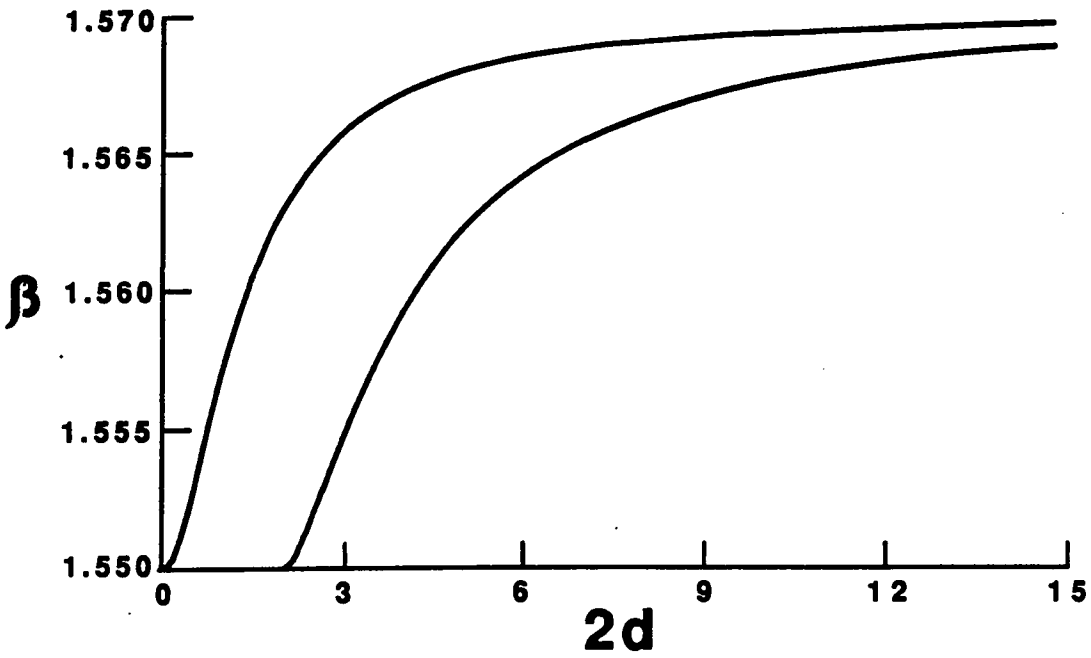

Fig. 2.2. Effective index β versus film thickness 2d for $n_1 = n_3 = 1.55$, $n_2 = 1.57$ and $\lambda = 1\mu m$. The curve on the left is the TE_0 mode and the other is the TE_1 mode.

we chose the refractive index of the cladding and substrate to be the same. By definition for a TE_m wave there are m zero crossings in the electric field profile. We see that as the film thickness 2d increases from zero the effective index increases from n_1, the refractive index of the cladding, up to n_2, the refractive index of the film. When the effective index β is near n_2 we have a tightly bound profile in the guide and as β goes down to n_1 the profile flattens out. For TE_0 waves at cutoff, $\beta \cong n_1$ and we have essentially a plane wave profile.

After choosing a suitable k_0, 2d and β combination that satisfy Eq. 2.15 we

can graph the three equations 2.12 - 2.14 for $x < -d$, $-d < x < d$ and $x > d$ respectively, to obtain a field profile of our guided wave. This field profile can provide visual information such as where the peak energy lies, the general size of the beam width, etc. Note that we have chosen to use TE_0 guided waves and henceforth our discussion will deal solely with this type of solution. The solutions to the wave equation for the linear case are exact solutions and upon propagation they remain unchanged in phase and amplitude. They are useful in understanding the basic phenomena of guided waves but do not provide information about propagation effects.

II.3 Nonlinear Guided Waves

II.3.a Introduction to Nonlinear Guided Waves

Using the same basic waveguide structure as discussed in the previous section only slightly modified we can study a completely different set of solutions to the wave equation. When one or more of the media chosen for the waveguide possesses a refractive index which depends on the field intensity we call the waveguide a nonlinear waveguide. In our study, we use a refractive index of the Kerr-type. For this type of media the refractive index depends on the modulus squared of the field amplitude (i.e. the field intensity) and we write

$$n^2(x,z) = n^2(x, |\mathcal{E}(x,z)|^2) = \begin{cases} n_1^2 + \alpha_1|\mathcal{E}(x,z)|^2 & x < -d \\ n_2^2 + \alpha_2|\mathcal{E}(x,z)|^2 & -d < x < d \\ n_3^2 + \alpha_3|\mathcal{E}(x,z)|^2 & x > d \end{cases} \tag{2.16}$$

where α_i is the nonlinear coefficient of the i^{th} medium [3]. This coefficient can be positive or negative; when α is greater than zero the nonlinearity is a self-focussing

nonlinearity and when it is negative we have a self-defocusing nonlinearity [17]. This intensity dependence of the refractive index must be included in the wave equation 2.10. We then obtain a nonlinear TE wave equation which has the form

$$\frac{\partial^2 \mathcal{E}}{\partial x^2} + 2ik_0\beta \frac{\partial \mathcal{E}}{\partial z} + k_0^2(n^2(x) - \beta^2)\mathcal{E} + k_0^2\alpha(x)|\mathcal{E}(x,z)|^2\mathcal{E} = 0. \qquad (2.17)$$

Using this nonlinear wave equation we can study the characteristics of a chosen nonlinear waveguide.

First we can obtain the stationary wave equation for TE guided waves by realizing that for stationary waves the field amplitude $\mathcal{E}(x,z)$ does not change under propagation, $\mathcal{E}(x,z) = \mathcal{E}(x)$. In this approach we see that $\partial\mathcal{E}/\partial z = 0$ and we are left with a stationary wave equation of the form:

$$\frac{d^2}{dx^2}\mathcal{E}_i(x) + k_0^2(n_i^2 + \alpha_i|\mathcal{E}_i(x)|^2 - \beta^2)\mathcal{E}_i(x) = 0. \qquad (2.18)$$

From this wave equation we can find exact solutions for nonlinear stationary waves by imposing the same boundary conditions on the field as for the linear case.

For our nonlinear waveguide model we use the same structure as in the linear case, however we choose the cladding to exhibit a Kerr-type nonlinearity, while the film and substrate are taken as linear, $\alpha_2 = \alpha_3 = 0$. We could choose a symmetric guide with both cladding and substrate nonlinear, however this would merely complicate our solutions and for our study the simple case above is quite sufficient. Results for the symmetric case can be found in Seaton et. al. [17].

We impose the previously discussed boundary conditions on the electric field to solve equation 2.18 and obtain the guided modes. Recall that for TE waves the

electric field and its transverse derivative are continuous across any interface. Our second boundary condition calls for limits on the electric field, that is for the wave to be physical $\mathcal{E}_1(-\infty) = 0$ and $\mathcal{E}_3(\infty) = 0$.

The exact solutions for the stationary TE waves with nonlinear cladding are

$$\mathcal{E}_1(x) = \frac{1}{2}\sqrt{\frac{2}{\alpha_1}}\,\frac{q_1}{\cosh[k_0 q_1(x + d - x_0)]}$$

for $\alpha_1 > 0$ (self-focusing case) or

$$\mathcal{E}_1(x) = \frac{1}{2}\sqrt{\frac{2}{|\alpha_1|}}\,\frac{q_1}{\sinh[k_0 q_1(x + d - x_0)]} \tag{2.19a}$$

for $\alpha_1 < 0$ (self-defocusing case).

$$\mathcal{E}_2(x) = \mathcal{E}_1(-d)\left[\cos(k_0 q_2(x + d)) + \frac{q_1}{q_2}\tanh^j(k_0 q_1 x_0)\,\sin(k_0 q_2(x + d))\right]$$

$$\mathcal{E}_2(x) = \mathcal{E}_1(-d)\left[\cosh(k_0 q_2(x + d)) + \frac{q_1}{q_2}\tanh^j(k_0 q_1 x_0)\,\sinh(k_0 q_2(x + d))\right] \tag{2.19b}$$

for $\beta^2 < n_2^2$ and $\beta^2 > n_2^2$, respectively, where $j = \pm 1$ is the sign of the nonlinearity, and

$$\mathcal{E}_3(x) = \mathcal{E}_2(d)\,\exp[-k_0 q_3(x - d)]. \tag{2.19c}$$

Here $q_i^2 = |\beta^2 - n_i^2|$ as before and x_0 is a constant which should be determined from the boundary conditions. This form of the nonlinear solution ensures that $\mathcal{E}(x)$ is continuous.

From these solutions we can find relationships between various parameters as before. By matching $\mathcal{E}$ and $\partial\mathcal{E}/\partial x$ at each interface we can find a relation between the effective index β and the product $2k_0 d$. This relation was found to be:

$$\tan(2k_0q_2d) = \left[1 + \frac{q_1}{q_3} \tanh^j(k_0q_1x_0) \right] / \left[\frac{q_2}{q_3} - \frac{q_1}{q_2} \tanh^j(k_0q_2x_0) \right]$$

$$\tanh(2k_0q_2d) = \left[1 + \frac{q_1}{q_3} \tanh^j(k_0q_1x_0) \right] / \left[-\frac{q_2}{q_3} - \frac{q_1}{q_2} \tanh^j(k_0q_2x_0) \right] \qquad (2.20)$$

for $\beta^2 < n_2^2$ and $\beta^2 > n_2^2$, respectively. The parameter x_0 can be found from β, $x_0 = x_0(\beta)$.

Of greater interest is the dispersion relation between the effective index β and the input guided wave flux S. This energy flux can be calculated by integrating the Poynting vector over the transverse dimension x [4].

$$S' = \frac{c\beta}{8\pi} \int_{-\infty}^{\infty} |\mathcal{E}(x)|^2 \, dx \qquad (2.21)$$

If we define

$$S_0' = \frac{cd}{4\pi|\alpha_1|} \qquad (2.22)$$

then the normalized flux is

$$S = \frac{S'}{S_0'} = \frac{\beta|\alpha_1|}{2d} \int_{-\infty}^{\infty} |\mathcal{E}(x)|^2 \, dx. \qquad (2.23)$$

Equation 2.23 gives the normalized energy flux per unit y dimension. This equation can be used to obtain the dispersion relation between β and S. The TE_0 dispersion curve for several thicknesses is shown in figure 2.3 for a self-focusing nonlinearity, $\alpha_1 > 0$. This configuration with a nonlinear self-focusing cladding will be used exclusively throughout this thesis. From figure 2.3 we see that for any thickness a wave can be guided (TE_0 is always above cutoff) and we also see for large enough thicknesses a local maximum in the guided wave power occurs. This happens

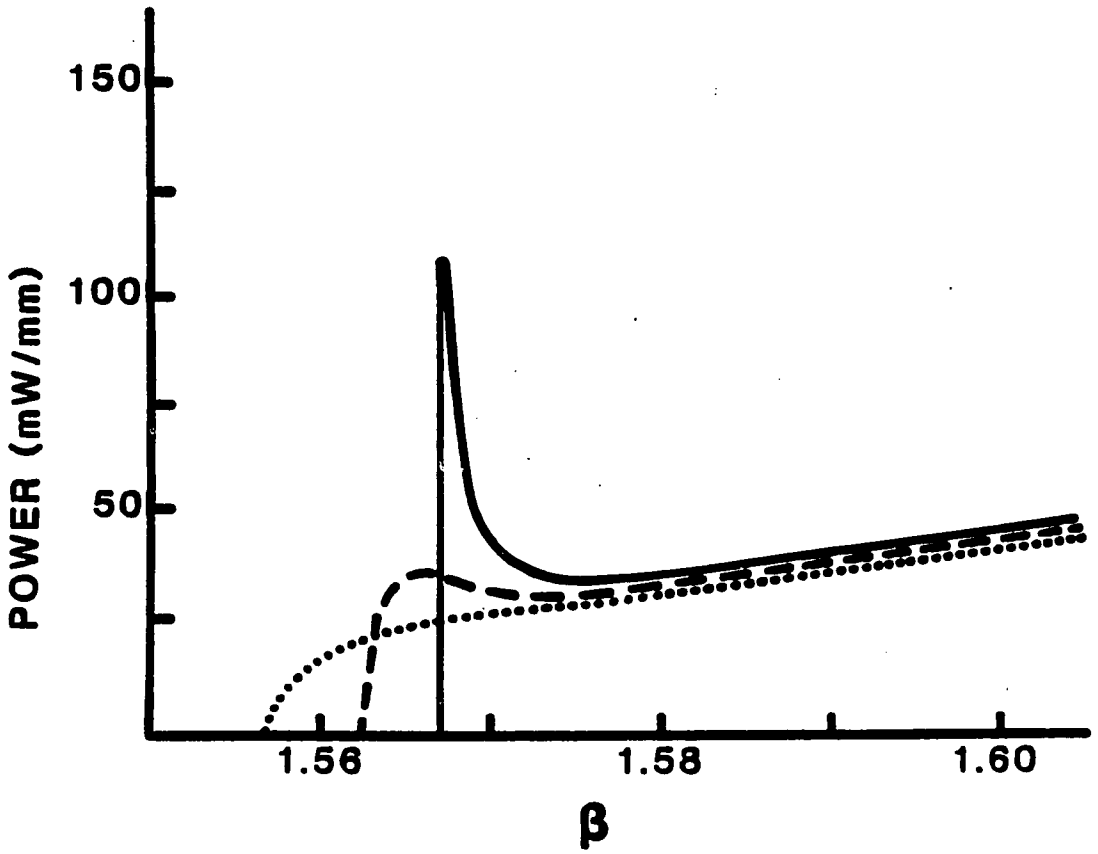

Fig. 2.3. TE_0 guided wave power versus effective index β for $n_1 = n_3 = 1.55$, $n_2 = 1.57$ and $\alpha_2 = 10^{-9}$ m^2/W for three different film thicknesses, $2d = 0.5$ μm (dotted line), $2d = 1.0$ μm (dashed line), $2d = 2.0$ μm (solid line).

because for thick films we can imagine two types of solutions for a given guided wave flux [17]. Basically, one is essentially a linear guided wave, and the other resembles a self-focused wave peaked in the nonlinear cladding. For very thick films the second solution barely sees the substrate and thus acts like a surface wave [28].

From the dispersion curve we see that depending on the flux the guided wave will have different β values and for some values of the input flux there are three different β values possible. Questions begin to arise about these solutions. The first

question that comes to mind is are all three possible nonlinear guided wave solutions stable under propagation? Secondly, can we excite these solutions using a Gaussian profile beam?

II.3.b Stability of Nonlinear Guided Waves

The stability analysis turns out to be quite complicated because equation 2.17 cannot be solved analytically. Instead the procedure used is to solve the wave equation for a steady state solution E(x) corresponding to one point on the dispersion curve and propagate this field down the guide using the split-step fast fourier transform method. After a reasonable propagation distance we compare the final field profile to the initial one. If this profile has not changed in shape or amplitude we call the solution a stable one. In using this method for determining stability it was found that the dispersion curve can be divided into three branches: two with positive slope ($dP/d\beta > 0$) and one with negative as shown in figure 2.4. A guided wave with initial profile obtained from the positively sloped branches of the dispersion curve was stable under propagation whereas a field from the negative branch was unstable. The two stable field profiles are also depicted in fig. 2.4 next to their respective branches.

Field evolution profiles for each of the three cases are displayed in figure 2.5. On branch I the field is centered in the guide and propagates unchanged acting essentially like a linear guided wave. In contrast, on branch II the field is localized in the nonlinear cladding and propagates unchanged like a surface polariton [17, 26]. However on the negatively sloped branch instability causes a wave-packet to break off and propagate into the nonlinear medium away from the guide. This wave packet propagates in the form of a self-focused spatial soliton. A soliton is a solitary

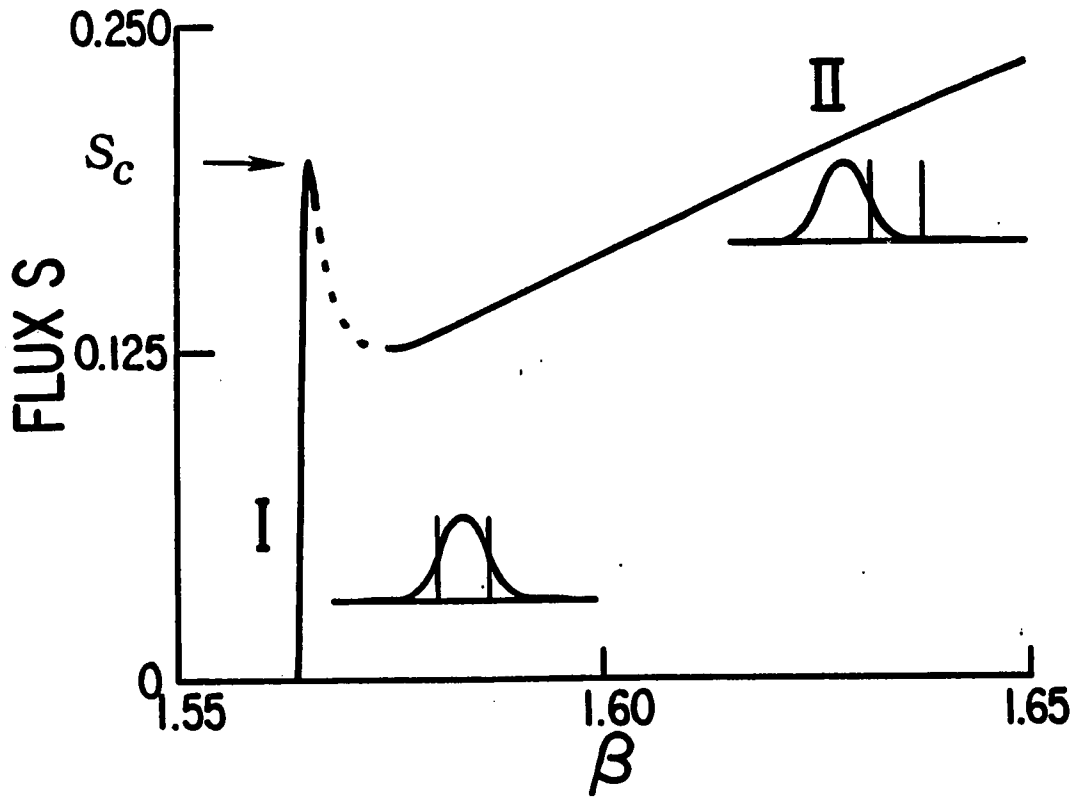

Fig. 2.4. Guided wave flux S versus effective index β for $n_1 = n_3 = 1.55$, $n_2 = 1.57$, $\alpha_2 = 10^{-2}$ and $2d = 8$. The solid and dashed lines indicate stable and unstable regions respectively, and the insets show the general nature of the nonlinear guided waves on the stable branches. S_c is the critical flux.

wave, i.e. a solution to the nonlinear wave equation that propagates unchanged in phase and amplitude, that is also stable [30, 31]. If both cladding and substrate are nonlinear the instability does not cause soliton emission but causes the profile peak to bounce back and forth in the guide. Soliton emission only occurred on this negatively sloped branch. We answered our first question by finding branches I and II stable but the intermediate one unstable.

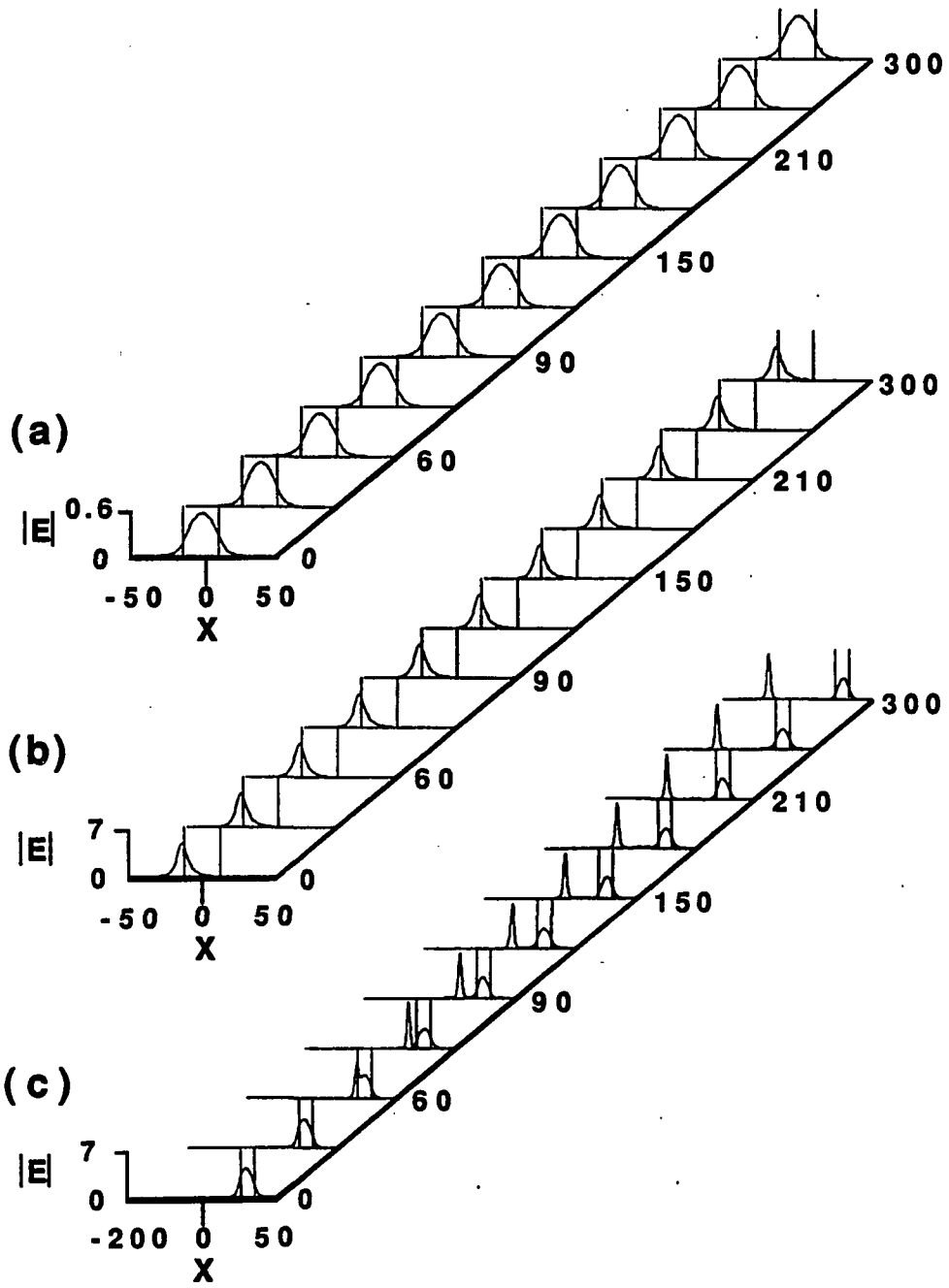

Fig. 2.5. Evolution of the field profiles in a nonlinear waveguide with the same parameters as in fig. 2.4, except 2d =12 μm, for (a) a branch I solution, (b) a branch II solution, (c) an unstable (negatively sloped) branch solution,. In this and all similar figures the vertical lines indicate the waveguide boundaries and the propagation coordinate is in units of free space wavelengths.

II.3.c Excitation of Nonlinear Guided Waves

In the first stability work the initial profile was always taken from the dispersion curve as a stationary solution to the wave equation and then propagated using the split step fast fourier transform routine [26, 28, 29]. Of interest though is how these nonlinear guided can waves be excited. One proposal was to see if they could be excited using a Gaussian beam. It was found by Wright et. al. that indeed either of the two stable solutions, branch I or branch II, could be excited using a Gaussian beam shaped similarly to the steady state solution and of reasonable input flux value [27]. By placing a beam of appropriate shape in the center of the guide a branch I solution was excited and by placing the beam near the cladding-film boundary the branch II solution could be excited. A solution on the negatively sloped branch cannot be excited which is understandable because it is an unstable branch. This Gaussian beam excitation work further supported the stability work. It showed that branches I and II are so stable that even a beam that was not exactly a steady state solution but similar could excite either of these two nonlinear guided waves.

Further work by Wright [32] explored the effect of fixing the profile to be that of a steady state linear solution but increasing the input flux above the critical flux S_c, the local maximum flux on the dispersion curve. Figure 2.6 shows the trapped flux after a reasonable propagation distance versus the input flux for a branch I solution. It was discovered that the discontinuities in this graph represent soliton emission from the guide. This thresholding behavior causes one or more soliton to be emitted when $S > S_c$, where the number of solitons emitted is approximately the integer part of S/S_c. In figure 2.7 we can observe this multi-soliton emission for various input flux values. After the appropriate number of

solitons are emitted a branch I solution is left in the guide. Theoretically, any input flux tailored and centered like a branch I solution will eventually result in excitation of a branch I solution with trapped flux between zero and the critical flux.

II.3.d More Questions About Nonlinear Guided Waves

In the stability and Gaussian beam excitation analysis of nonlinear guided waves the answers to our initial questions were found. Only positively sloped branches of the dispersion curve, $dP/d\beta > 0$, were found stable. These stable solutions can be excited using appropriately shaped and placed Gaussian beams. More importantly new questions arose about these nonlinear guided waves. We assumed ideal conditions above. What happens to nonlinear guided waves if the system is not lossless?

In my thesis work I first studied the effect absorption has on nonlinear guided waves. Secondly, I studied the phenomenon of soliton emission and how it is affected by nonideal conditions.

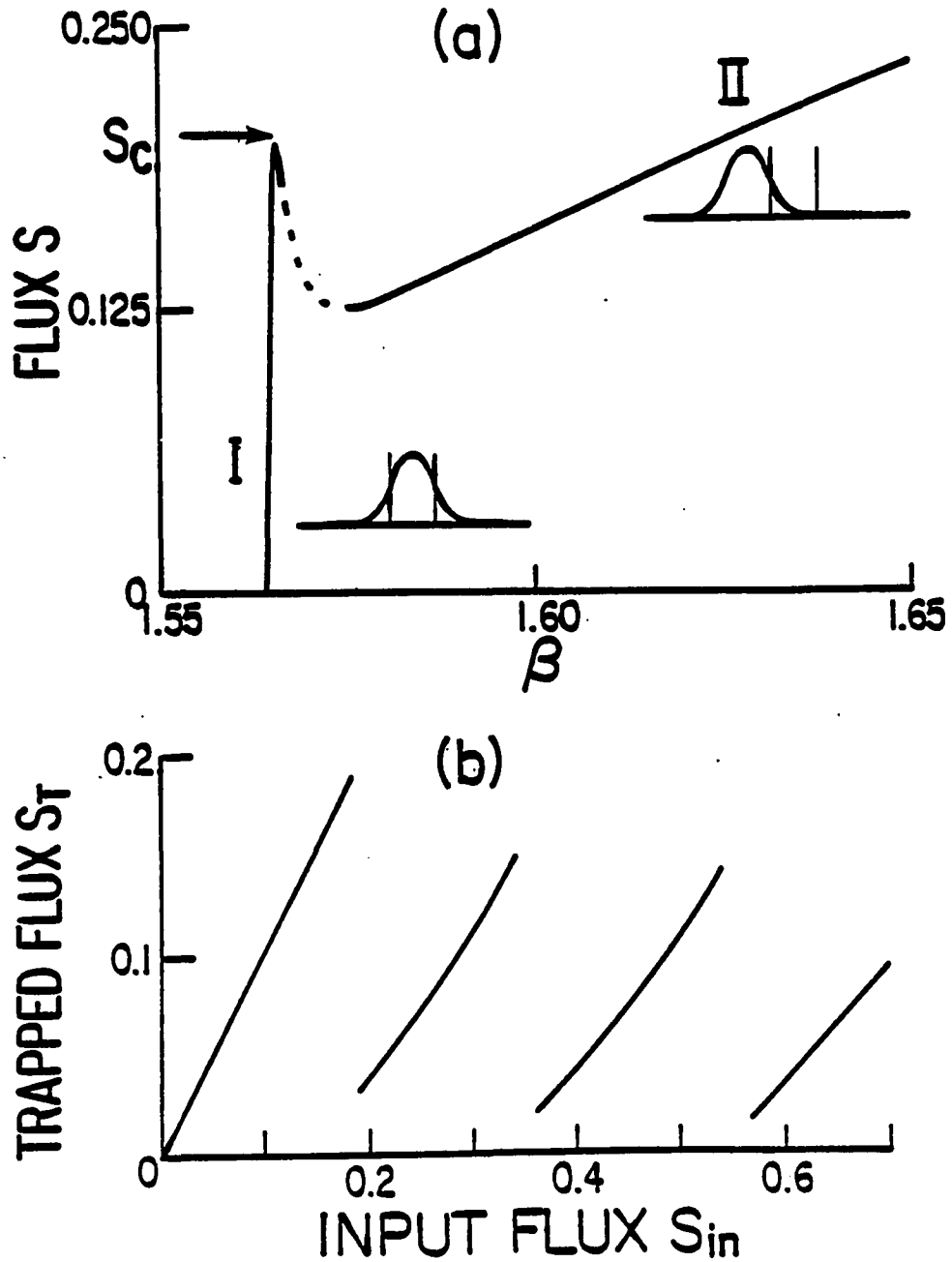

Fig. 2.6. (a) Same as fig. 2.4. (b) Flux trapped in the guide S_T versus the input flux S_{in}. The input beam profile is held fixed as the linear TE_0 guided mode.

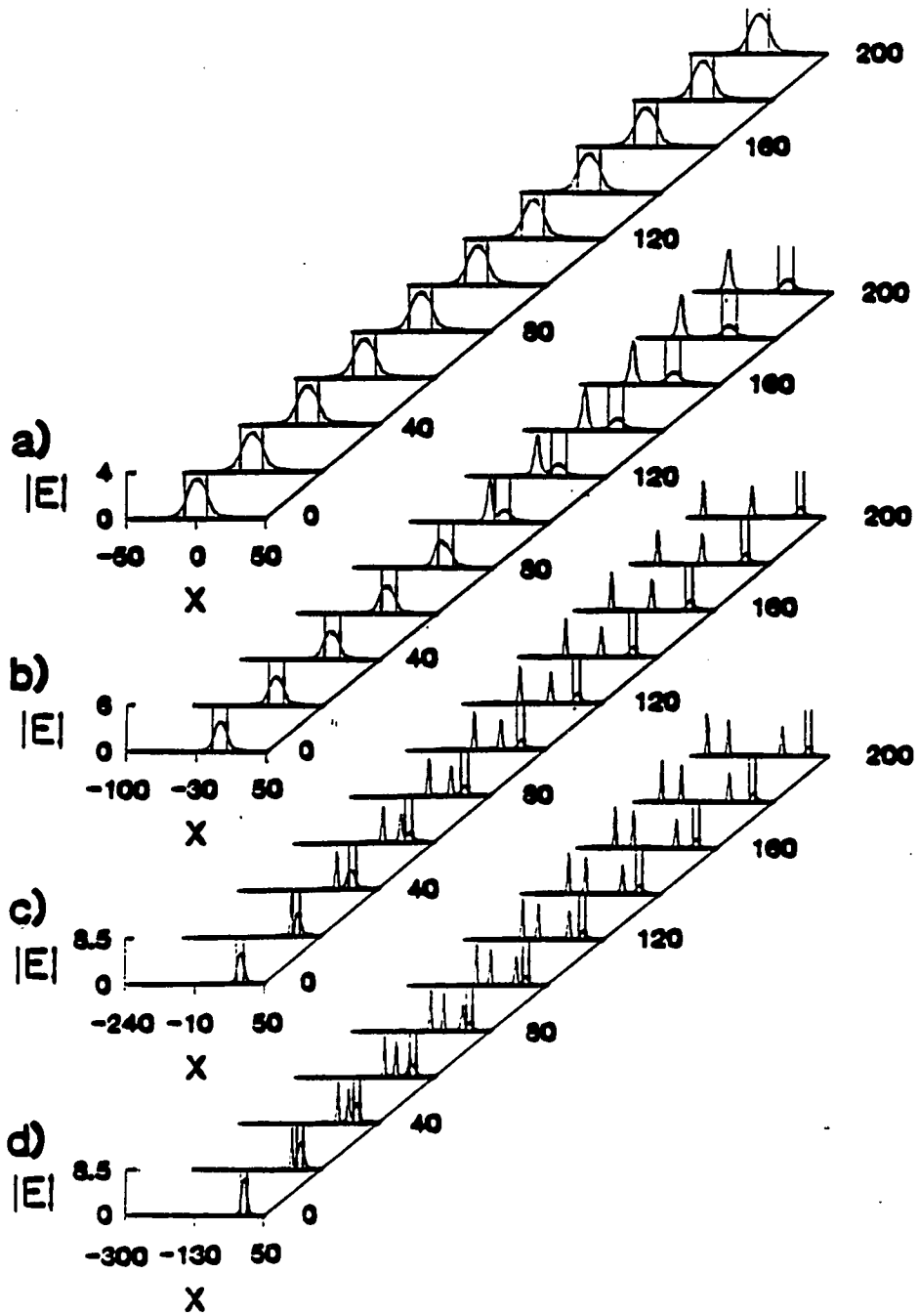

Fig. 2.7. Evolution of the input fields for flux levels (a) 0.15, (b) 0.2, (c) 0.4, (d) 0.6.

III EFFECTS OF ABSORPTION ON NONLINEAR GUIDED WAVES

III.1 Absorption in the Nonlinear Wave Equation

In the previous section our analysis using the wave equation to obtain stationary guided wave solutions applied only to the lossless case and did not take into account the absorption that is present in waveguides. However some absorption is present in all waveguides and can be significant for nonlinear media [33]. Using the beam propagation method we investigated the effects of linear absorption on the TE_0 nonlinear guided waves. We found that the distribution of this absorption in the waveguide had profound effects on the propagation of the nonlinear guided waves obtained from the lossless case.

The linear absorption varies transversely across the guide due to the different media it is composed of. If we characterize this absorption profile using $\Gamma(x) = \Gamma_i$ where, as before, $i = 1, 2, 3$ for the cladding, film and substrate, we rewrite the nonlinear wave equation 2.17 as

$$\frac{\partial^2 \mathcal{E}}{\partial x^2} + 2ik_0\beta \frac{\partial \mathcal{E}}{\partial z} + k_0^2(n^2(x)+\alpha(x)|\mathcal{E}(x,z)|^2-\beta^2)\mathcal{E} + ik_0\beta\Gamma(x)\mathcal{E} = 0 \qquad (3.1)$$

Here Γ_i is an absorption coefficient. This new nonlinear wave equation can be used as before to study the effect absorption has on the propagation and the excitation of nonlinear guided waves [34]. With the split step fast fourier transform method of propagation we can determine the electric field profile of the nonlinear guided waves at various points of its propagation. By comparing the lossless profiles to those where absorption is included we can investigate how absorption affects nonlinear

guided waves.

III.2 Effects of Absorption on the Propagation of Nonlinear Guided Waves

Two different cases of absorption profiles were of interest to us, namely, lower absorption in the film than in the bounding media and vice-versa. The wave guide has the same configuration as before with only the cladding nonlinear. In this section, for simplicity we chose the absorption in the cladding and substrate to be the same, $\Gamma_1 = \Gamma_3$. We used large but not unrealistic absorption coefficients to display clearly the differences between the two cases. Similar results would be obtained for lower values but require larger propagation lengths. The propagation lengths used were chosen to be a couple of absorption lengths for the larger of Γ_1 or Γ_2.

For the first case we chose the absorption in the cladding and substrate to be greater than that in the film, $\Gamma_1 = \Gamma_3 > \Gamma_2$. Specifically we used $k_0\Gamma_1 = 10^{-2}$ and $k_0\Gamma_2 = 10^{-3}$. We were interested in two parameters, the normalized guided wave flux S(z) and the effective absorption that the guided wave sees $\Gamma_e(z)$. Note that both these quantities depend on the propagation distance and can be given by

$$S(z) = \frac{\beta|\alpha_1|}{2d} N(z) \tag{3.2}$$

$$\Gamma_e(z) = \frac{1}{N(z)} \int_{-\infty}^{\infty} dx\, \Gamma(x)|\mathcal{G}(x,z)|^2 \tag{3.3}$$

where

$$N(z) = \int_{-\infty}^{\infty} dx|\mathcal{G}(x,z)|^2$$

Using the propagation routine with our new wave equation 3.1 and the above

relations we can calculate the normalized flux and the effective index of the guided wave as it evolves.

We chose three different stationary solutions to propagate in our study. The first and second solutions are from branches I and II of the dispersion curve, fig. 2.5, respectively, both having a normalized input flux of S = 0.13. The third solution is one from branch II with an input flux of S = 0.5. In figure 3.1(a) the evolution of the flux versus propagation distance is displayed for the above three cases and figure 3.1(b) shows the effective absorption versus flux for these cases.

In these two figures we notice several details. Curve I in figure 3.1(a) displays the least absorption. This is natural because as a branch I solution it is concentrated mainly in the film [17] where the least absorption is. As evidenced in curve I of figure 3.1(b) where Γ_e is essentially constant, this field profile propagates almost unchanged but decays in height exponentially $\cong \exp(-\Gamma_2 z)$. Curves II and III obtained for the branch II solutions are more drastic than curve I as is expected because they are localized in the nonlinear cladding where the absorption is greatest. In figure 3.1(a) the flux decays more strongly for the branch II solutions with curve III showing stronger decay than II because the higher flux guided wave is localized further into the cladding than the lower one [17]. Figure 3.1(b) shows similar structure for curves II and III. Both curves have a high effective absorption initially and decrease as the solution propagates (note that the solution evolves from high flux to low flux as it propagates). Of interest is that the curve III solution actually starts at $\Gamma_e \cong \Gamma_1$; this is because it is localized almost entirely in the cladding. As both of these branch II solutions propagate the self-focused peak evolves toward the film and eventually penetrates into it. The effective absorption decreases with the propagation because more of the profile is inside the film. The small oscillation in fig. 3.1(b)

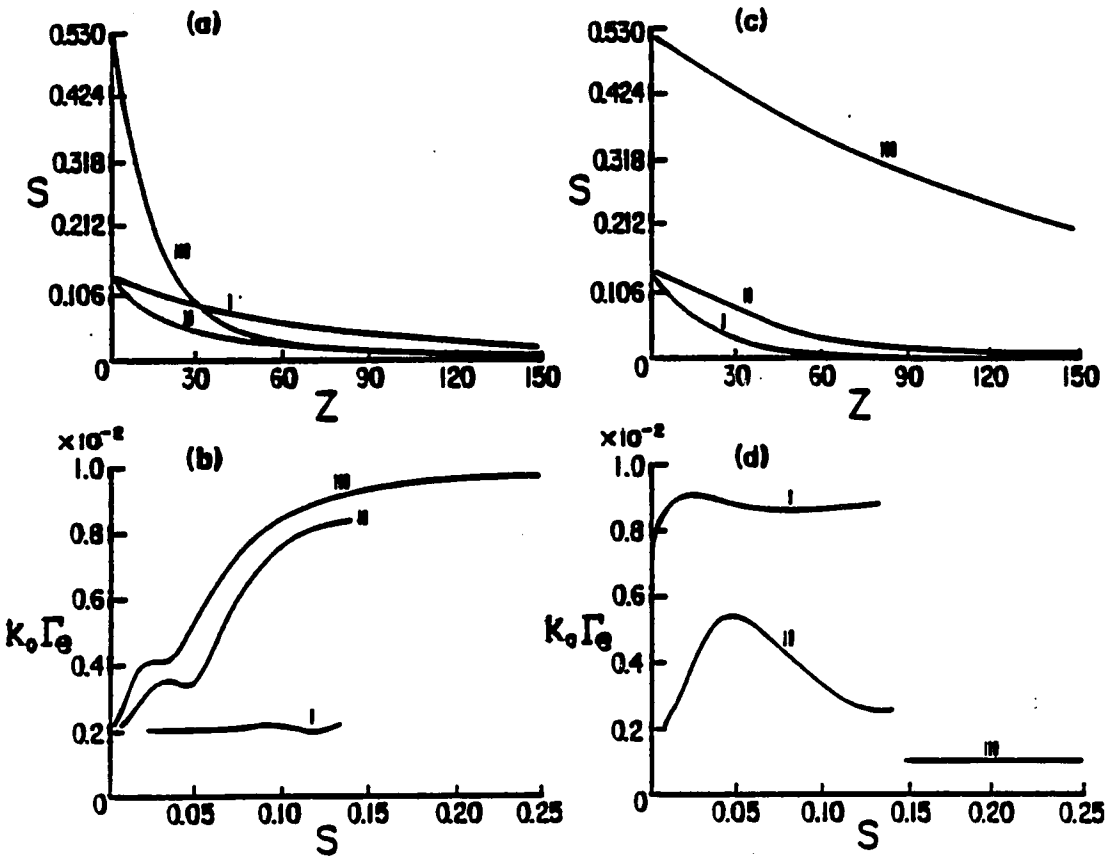

Fig. 3.1. (a) Wave flux S versus propagation distance z and (b) effective absorption $k_0\Gamma_e$ versus flux S, for $k_0\Gamma_1 = k_0\Gamma_3 = 10^{-2}$, $k_0\Gamma_2 = 10^{-3}$ and three different initial nonlinear guided waves from fig. 2.4. Curves I and II correspond to branch I and II type solutions, respectively, of the same initial flux S = 0.13. Curve III corresponds to a branch II solution of initial flux S = 0.5. Figs. (c) and (d) are the same as (a) and (b) except $k_0\Gamma_1 = k_0\Gamma_3 = 10^{-3}$ and $k_0\Gamma_2 = 10^{-2}$.

occurs because after the peak penetrates into the film the inertia of the wave causes it to be temporarily drawn back toward the cladding. After this oscillation the wave evolves toward a branch I solution and, as we see from figure 3.1(b), Γ_e, the effective absorption, decreases toward the constant Γ_2, the absorption of the film.

Figure 3.2 displays the evolution profiles of these three cases. Note how in fig. 3.2(a) the branch I profile decays but does not move around in the guide. In fig.

3.2(b) the curve II profile moves into the film and decays. As evidenced between the sixth and seventh profiles, the peak moves back toward the cladding causing the small oscillation we mentioned in fig. 3.1(b). The last evolution plot, fig. 3.2(c), is for the higher flux branch II solution. We observe how quickly the flux is dissipated (note the change of scale for the propagation distance). This quick loss of energy can also be seen in fig. 3.1(a), curve III.

For curves II and III, figs. 3.2(b,c), we see that the self-focussed peak is attracted toward the film which is the region of lower absorption. We can say that the absorptive profile actually possesses focusing properties. If we consider an input field with its peak located in the film we realize that this field is absorbed least in the film and more strongly in the bounding media. Thus, our configuration produces a focusing of the local field in the film. It is this absorptive focusing that attracts the field toward the film in the branch II cases.

One final detail to recognize is that in fig. 3.1(b) curves II and III show similar features however they do not overlap. If propagation effects were ignored and the field distribution assumed to adiabatically evolve along the dispersion curve these two curves would be coincident. We realize from their difference that propagation cannot be ignored in the present problem [35].

Our second study for this section uses higher absorption in the film than in the cladding and substrate, $k_0\Gamma_2 = 10^{-2}$ and $k_0\Gamma_1 = k_0\Gamma_3 = 10^{-3}$. Using the same three stationary solutions as above for this new guide configuration we obtain drastically different results. Figures 3.1(c,d) correspond to 3.1(a,b) for our new absorption profile. We see from fig. 3.1(c) that the curve III solution suffers least from absorption, whereas the curve I solution suffers most. This again is understandable in that the branch II solution of higher flux is localized furthest into the cladding

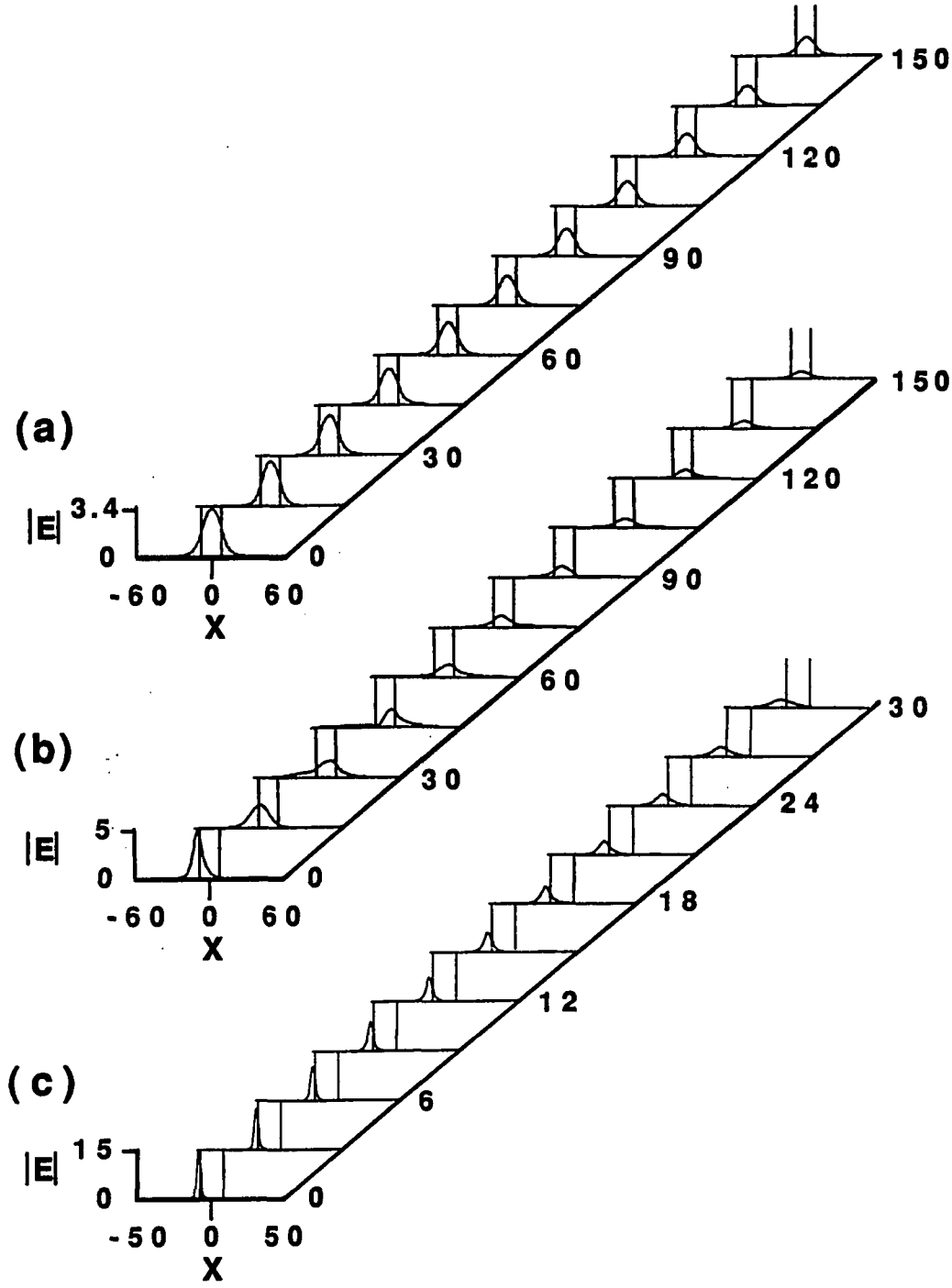

Fig. 3.2. Evolution of the field profiles for the results corresponding to figs. 3.1(a,b) for (a) curve I, (b) curve II, (c) curve III. Note the change of scale in the propagation distance.

where the absorption is lowest but the branch I solution is in the film where the absorption is greatest. Using the focusing argument from above we would expect the film being of higher absorption to repel the field and the cladding and substrate to attract it. In this case it is the curve III solution in fig. 3.1(d) for which the effective absorption Γ_e stays constant and equal to Γ_1. The evolution of the field

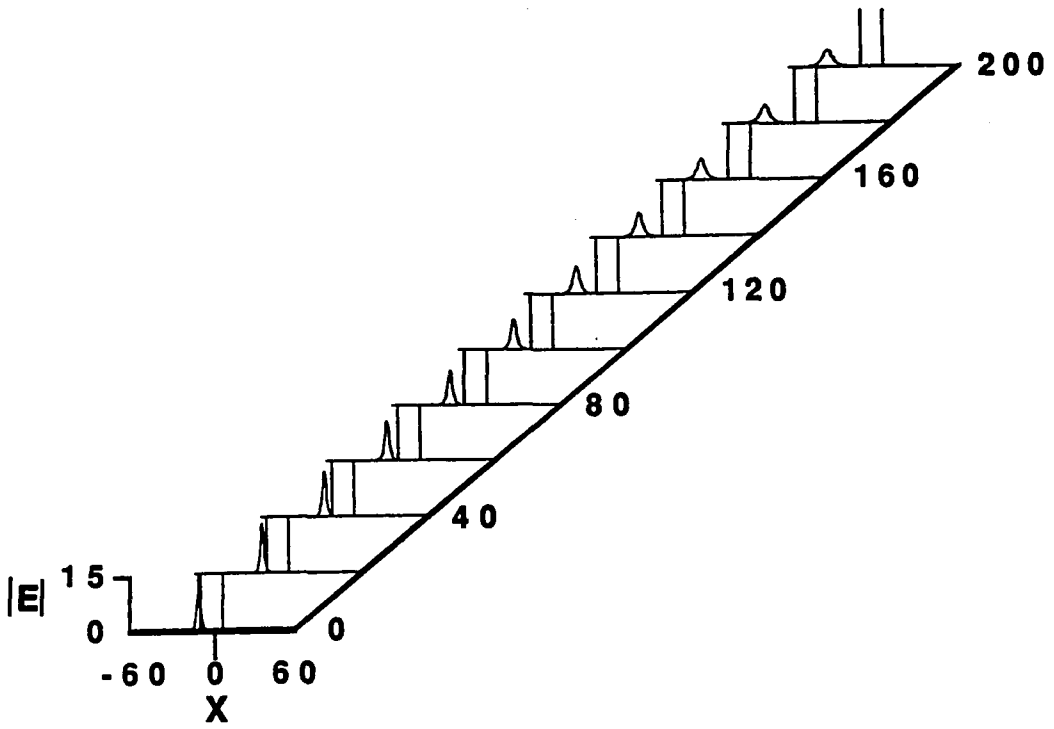

Fig. 3.3. Evolution of the field profile for results corresponding to figs. 3.1(c,d) curve III.

profile versus propagation distance is shown in fig. 3.3 for this solution. The initial field is far enough away from the film that it can break away from the waveguide and move further into the cladding. As it evolves away from the film it decays and broadens.

The initial field profiles and the profiles after seventy-five wavelengths

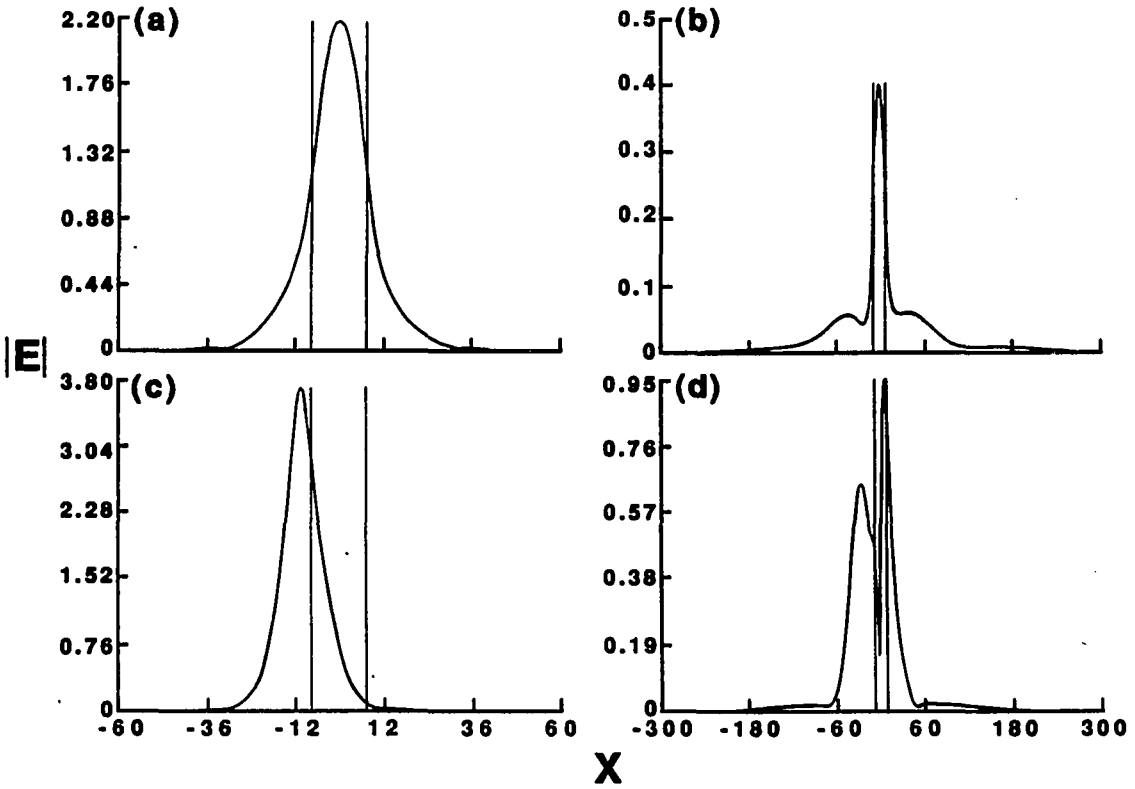

Fig. 3.4. (a) and (c) are input waves used to generate curves I and II of figs. 3.1(c,d), respectively. (b) and (d) are their respective field profiles after 75 wavelengths propagation.

propagation are shown in figs. 3.4(a-d) for the solutions of curves I and II of figs. 3.1(c,d). We see in both cases the field being attracted to the cladding and substrate. For curve II the field initially moves toward the film and so its effective absorption increases, fig. 3.1(d). As it propagates further the field evolves into the cladding and substrate in the form of side-waves which propagate away from the film and the effective absorption begins to decrease with decreasing flux (or increasing propagation distance). These side-waves can be seen in fig. 3.4(d). In the case of curve I of fig. 3.1(d) the branch I solution is localized mainly in the film where the

greatest absorption is. It therefore encounters a high effective absorption, $\Gamma_e \cong \Gamma_2$, at the beginning of its propagation. Eventually the field radiates out into the cladding and substrate, fig. 3.4(b), leading to the decrease in Γ_e of fig. 3.1(d).

This study's results demonstrate that the effect of absorption on TE_0 nonlinear guided waves depends strongly on the absorption profile. The field is always attracted to regions of lower absorption and it decays under propagation. Again the absorption coefficients used were large but not unrealistic and for smaller absorption coefficients the effects are similar but not so strong for the same propagation distance.

III.3 Effects of Absorption on the Excitation of Nonlinear Guided Waves

In the previous section we employed absorption in all three media, the cladding, film and substrate. In realistic waveguides with a nonlinear cladding and linear film and substrate it is reasonable that only the cladding will exhibit significant absorption [33]. In fact, it is absorption that is responsible for the nonlinear refractive index. The resonant interaction between the field and the nonlinear media requires absorption. We will approximate it as linear absorption. On the other hand, the field interacts nonresonantly with linear media and thus the absorption is low for this media. Irregularities in the waveguide give rise to unavoidable scattering losses but they are small compared to the absorption due to the nonlinearity and so we will neglect them in this section.

We discussed in section II.3.c how a Gaussian beam appropriately tailored and placed can be used to excite any stable TE_0 nonlinear guided wave in the lossless case. It is of interest to know if this is still true in the presence of absorption. We chose a waveguide where the cladding was nonlinear and displayed absorption, but

the film and substrate were linear and lossless. It is important to recognize that real nonlinear guided waves do not exist in the presence of absorption but it was hoped that fields resembling these waves would survive the presence of absorption and be excited in the nonlinear waveguide.

To investigate the excitation of these waves in the presence of absorption we solved eq. 3.1 with initial data corresponding to a collimated Gaussian input beam.

$$E_{in}(x,0) = A\, e^{(x-x_0)^2/\omega_0^2} \tag{3.4}$$

Here A is used to adjust the input beam flux, x_0 is the displacement of the input beam center from the guide center and ω_0 is the Gaussian spot size. As explained by Wright [27], the above procedure corresponds to end-firing a Gaussian beam onto the nonlinear guided wave. We were interested in exciting a branch II solution at the cladding-film boundary and so we chose an input flux of $S_{in} = 0.155$, a displacement of $x_0 = -10.6$ and a spot size of $\omega_0 = 4.0$. Using these parameters in eq. 3.4 to solve eq. 3.1 in our propagation routine, we found branch II nonlinear guided waves could successfully be excited in the presence of absorption. The input wave was taken as the nonlinear guided wave in the absence of absorption. We chose a propagation distance of 300 wavelengths and investigated three different absorption coefficients, $k_0\Gamma_1 = 10^{-5}, 10^{-4}, 10^{-3}$. Plotted in fig. 3.5 is the flux as a function of propagation distance for these three coefficients. In figs. 3.6(a-c) we display the evolution of the field profiles. We can see in figs. 3.6(a,b) that a wave resembling the nonlinear guided wave does indeed survive the absorption for $k_0\Gamma_1 = 10^{-5}$ and $k_0\Gamma_1 = 10^{-4}$. However for $k_0\Gamma_1 = 10^{-3}$ the absorption is too great for this to occur and the field evolves toward and eventually settles into the film. This phenomena is evident in

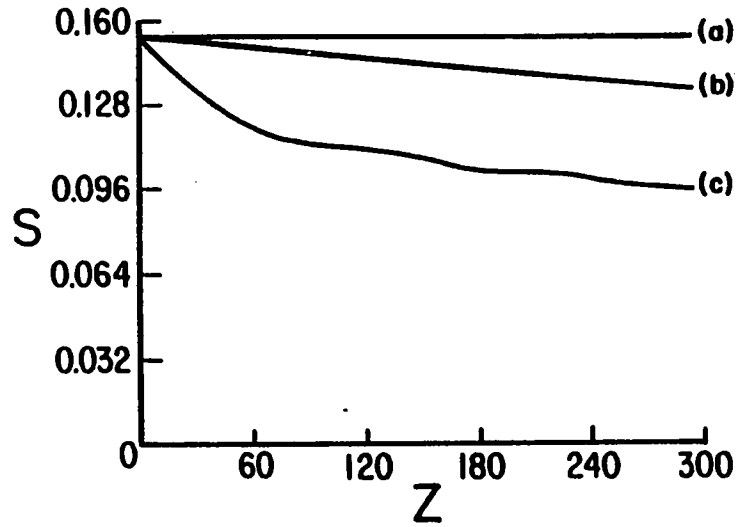

Fig. 3.5. Evolution of the wave flux S versus propagation distance z for the same input wave and $k_0\Gamma_1$ = (a) 10^{-5}, (b) 10^{-4}, (c) 10^{-3}. The input wave is a displaced Gaussian.

fig. 3.5(c) where the flux falls off rapidly at first and once the field moves inside the film the slope of the curve 3.5(c) flattens out.

Again we have shown that absorption in a nonlinear waveguide reduces the efficiency or limits the useful device length of the guide. If the absorption is low enough the results obtained resemble the lossless case, but for higher absorption coefficients the loss needs to be taken into account when designing the device.

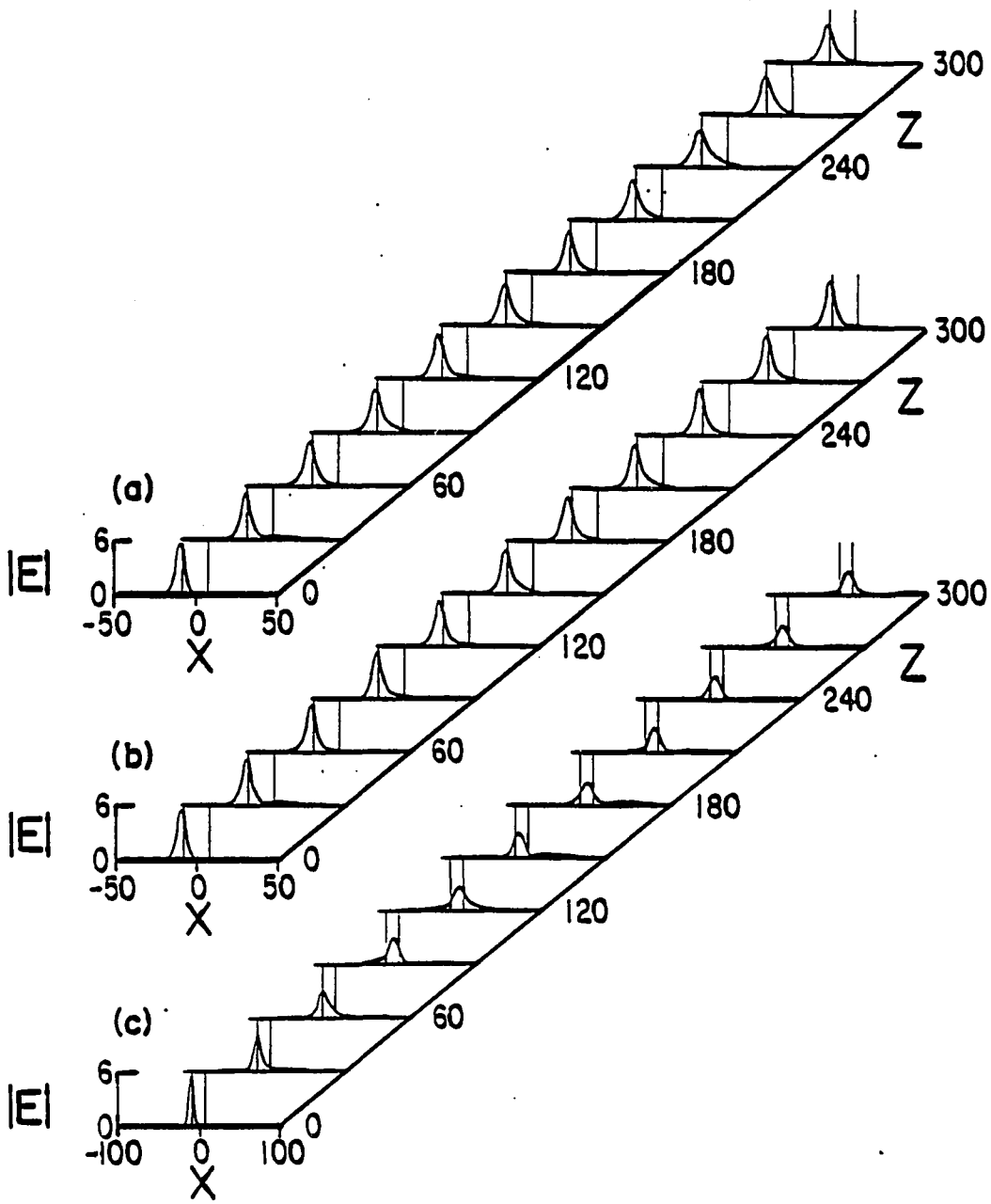

Fig. 3.6. Evolution of the field profiles corresponding to figs. 3.5(a, b, c), respectively.

IV SOLITON EMISSION UNDER NONIDEAL CONDITIONS

IV.1 Soliton Emission from a Nonlinear Waveguide

In section II.3.c we discussed briefly the ability to excite a nonlinear guided wave using a suitable Gaussian input beam. We also mentioned that multi-soliton emission can occur when the input flux of a linear guided wave solution exceeds the critical flux of that guide's dispersion curve. Here we will use a collimated Gaussian input beam of flux greater than the critical flux to produce soliton emission. The previous work on multi-soliton emission by Wright [32] assumed ideal conditions, i.e. the guide was lossless, the input beam was exactly aligned, the nonlinearity was unsaturable. (See figs. 2.7 and 2.8). It is important to know how nonideal conditions affect the occurrence of soliton emission.

In this study we looked at several complications to the ideal case to determine whether the phenomenon of soliton emission is resilient enough to be searched for seriously in a laboratory experiment. We performed a numerical study of the effects of linear absorption, input beam misalignments and nonlinear saturation on soliton emission from a nonlinear guided wave [36]. Again we must note that in the presence of absorption no true soliton solutions of the nonlinear wave equation exist, but it is hoped that results reminiscent of the lossless case will survive.

We solved the nonlinear wave equation that included the absorption coefficient, eq. 3.1, with initial data corresponding to a Gaussian input beam of the form

$$E(x,0) = A \exp\{i[Q(x - x_0)^2/2 + \kappa x]\} \qquad (4.1)$$

Here, as before, A is used to adjust the input beam flux, x_0 is the displacement of the input beam peak from the guide center and ω_0 is the Gaussian spot size. $\kappa = \sin\theta$ accounts for the fact that the input beam may travel at an angle θ with respect to the z axis. For $|\theta| \ll 1$, $\kappa \cong \theta$. Q is the input complex beam parameter given by

$$Q = \frac{1}{R} + \frac{2i}{k_0^2\omega_0^2}, \tag{4.2}$$

where R is the input beam radius of curvature.

By using eq. 4.1 as the input beam and adjusting the appropriate parameters we studied the effect of the various complications on the nonlinear guided wave. In order to fully understand how the various complications affect the wave we decided to apply each one independently to the same basic configuration. To do so we held several of the parameter values fixed throughout this study and varied only one parameter in each case. Our fixed parameters were $n_1 = n_3 = 1.55$, $n_2 = 1.57$, $\alpha_1 = 0.01$, $\alpha_2 = \alpha_3 = 0.0$. As before the film and substrate are assumed lossless. The input beam Gaussian spot size was set at $k_0\omega_0 = 10$. The following sections discuss separately the effects of absorption, input beam misalignment, and nonlinear saturation on soliton emission.

IV.2 Effects of Linear Absorption on Soliton Emission

In this section we discuss the effects of linear absorption on soliton emission. Again no true soliton exists in the presence of absorption so we looked for results reminiscent of the lossless case. The absorption in the nonlinear media is in general much greater than that in the linear therefore, in this study, we chose to include only this nonlinear absorption. Figure 4.1 displays the results of this absorption study.

We used an input flux of $S_{in} = 0.22$, which gave us single-soliton emission in the lossless case, and varied the absorption coefficient in the cladding, Γ_1. We see that for $k_0\Gamma_1 = 10^{-4}$ in fig. 4.1(a) the effects of linear absorption are small over the propagation distance considered. The soliton that is emitted propagates visibly unchanged. For $k_0\Gamma_1 = 10^{-3}$ in fig. 4.1(b) the effect of absorption is more drastic. Although the localized wave-packet is emitted it decays and broadens as it evolves away from the cladding-film interface. Though not visibly apparent, this wave-packet's velocity away from the interface decreases. Finally, for $k_0\Gamma_1 = 10^{-2}$ in fig. 4.1(c) no wave-packet is emitted. The absorption here immediately reduces the energy of the guided wave before a soliton can be emitted and it continues to drain the energy from the guided wave.

We realize that localized wave-packet emission still occurs if the absorption is small, but this absorption limits the useful device length and if the absorption is large no emission occurs. Similar results are obtained for input flux levels that produce multi-soliton emission in the lossless case. There also, increasing the absorption reduces the number of waves emitted and eventually prohibits emission altogether.

IV.3 Effects of Input Beam Misalignment on Soliton Emission

In this section we study the effects of input beam misalignment on soliton emission. In particular, we looked at three types of misalignment, noncollimated beam, transverse displacement and angular displacement. All three complications are tolerated so that soliton emission still occurs however, in general, they do produce significant amounts of radiation. In contrast, radiation in the ideal case is negligible [32]. We will mention only briefly the results of the test with a noncollimated beam as they were uninteresting compared to the other misalignments. On the other hand,

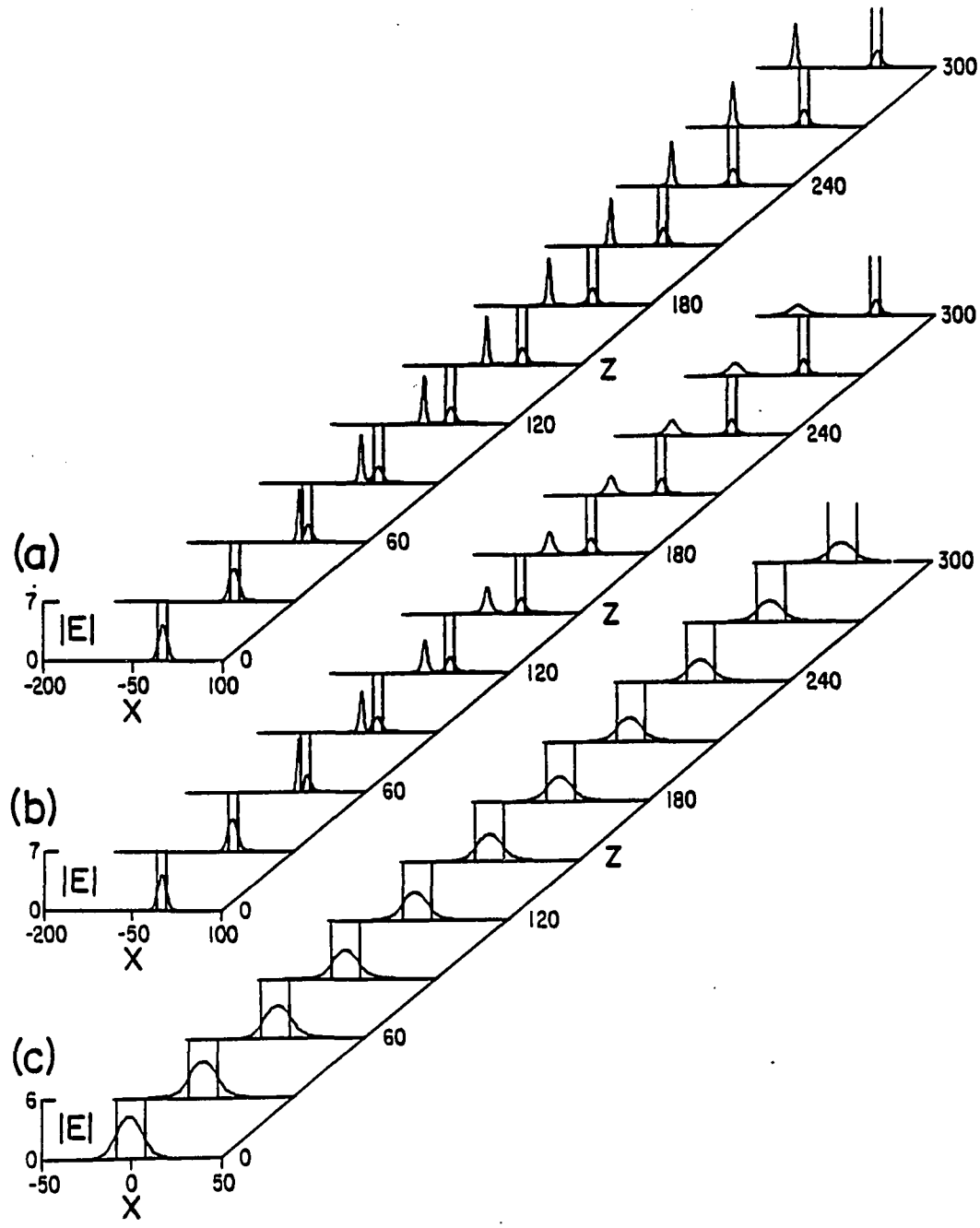

Fig. 4.1. Soliton emission in the presence of absorption. The input flux in all cases is $S_{in} = 0.22$ and the absorption coefficient $k_0\Gamma_1$ = (a) 10^{-4}, (b) 10^{-3}, (c) 10^{-2}.

we will present results and figures for the cases of transverse and angular displacements. The former example illustrates how resilient soliton emission is to input beam misalignment, and the latter illustrates how a misalignment need not produce a significant amount of radiation.

In the case of transverse displacement we again considered an input beam of flux $S_{in} = 0.22$, but displaced the center of the beam by eight units. Figures 4.2(a,b) show the initial beam profile displaced into the substrate and the beam profile after propagation of 100 free space wavelengths, respectively. We see that soliton emission still occurs, however a significant radiation component is clearly present. At first it seems unusual that soliton emission can occur when the beam is displaced so far away from the nonlinear media, but if we think of the guide as a focusing medium drawing the input toward the film we can understand what happens. Once the motion has commenced the field moves not only into the film but also closer to the cladding, the nonlinear media. When close enough to the cladding, soliton emission can occur just as it does when the field is initially in the film. From this transverse displacement example we discover that soliton emission is highly resilient against input beam misalignments.

Now we consider the effect of angular displacement on soliton emission. We investigated the possibility that the input beam does not enter the guide at normal incidence but at a slight angle θ. The effects of angular displacement are depicted in fig. 4.3 where again we used $S_{in} = 0.22$. From fig. 4.3(a) where the input beam was directed up into the nonlinear cladding we see that soliton emission occurs with negligible radiation. In contrast fig. 4.3(b) shows a frame from the evolution plot where the input beam was directed down into the linear substrate. We see here that although soliton emission still occurs significant amounts of radiation are produced.

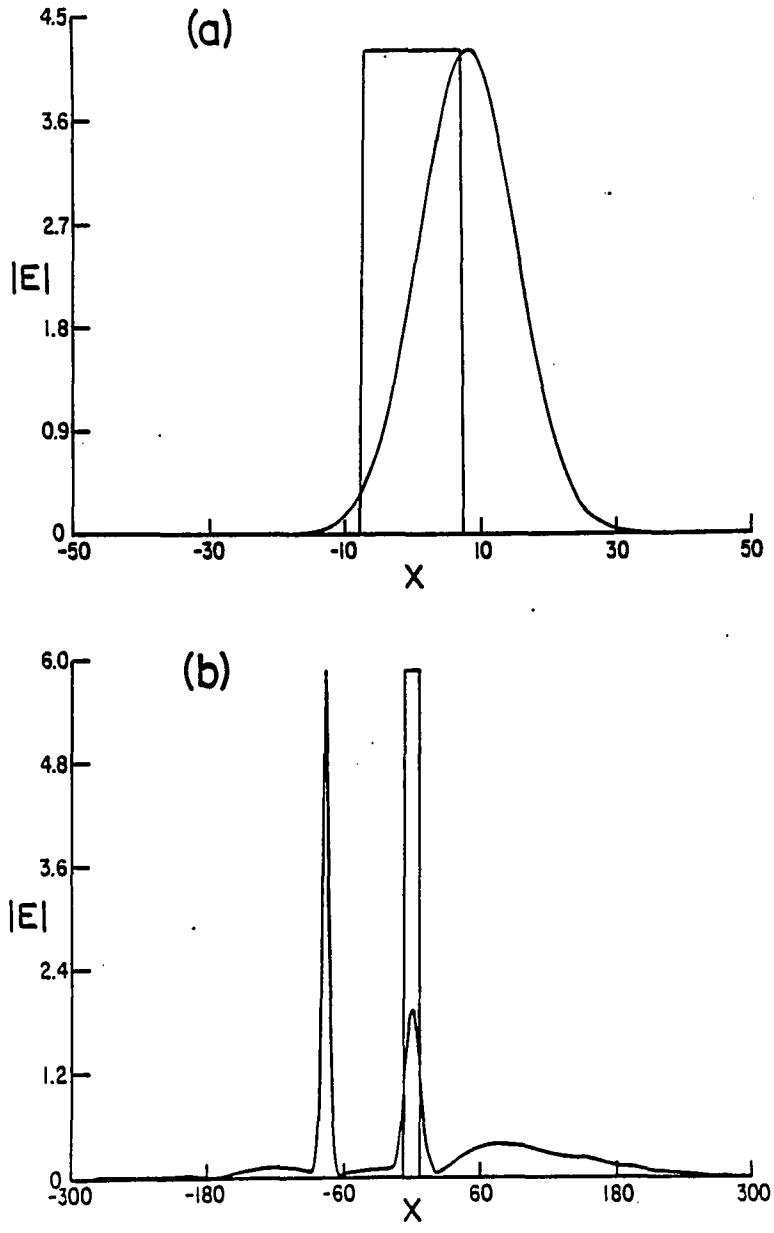

Fig. 4.2. Soliton emission in the presence of a transverse displacement $x_0 = 8$ for an input flux $S_{in} = 0.22$; (a) the input profile, (b) the field after 100 wavelengths propagation.

Here also it may seem unusual that soliton emission can occur, but again if we think of the film as an attractive potential we see that it can confine the field and produce

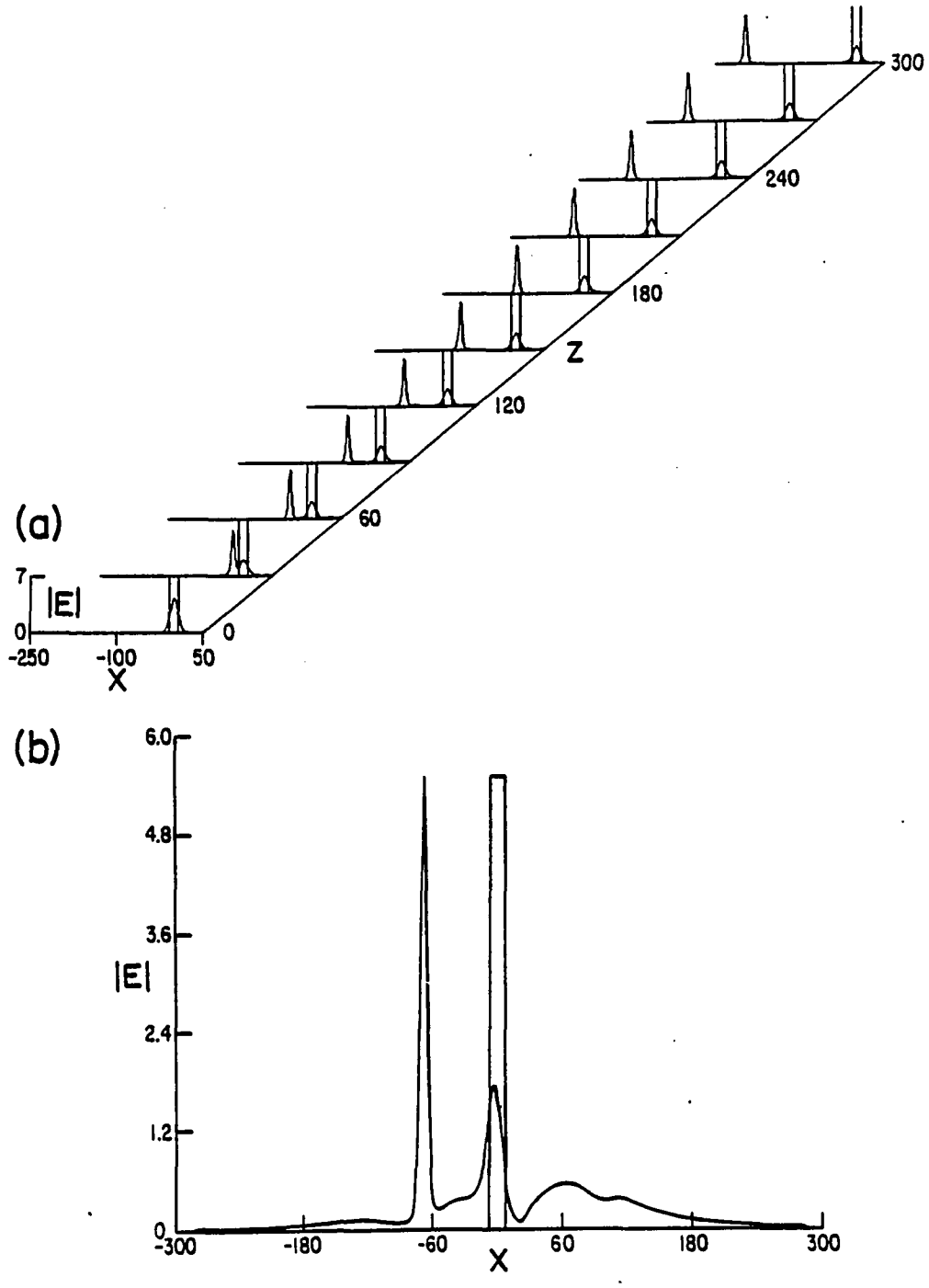

Fig. 4.3. Soliton emission in the presence of an angular displacement for an input flux S_{in} = 0.22 and (a) θ = -0.1, (b) θ = +0.1.

a soliton. However, if the angular displacement is large enough to overcome the confinement the wave can escape into the linear substrate.

Here we realize that soliton emission can occur when the input beam is misaligned but is usually accompanied by large amounts of radiation. For some misalignments though negligible radiation is produced. Whether the soliton could be detected depends, in part, on the amount of radiation produced.

IV.4 Effects of Nonlinear Saturation on Soliton Emission

To investigate the effect of saturation on soliton emission we must include a saturation parameter $\mathcal{X}$ in our nonlinear refractive index. The refractive index profile can now be written [36]

$$n^2(x,|\mathcal{E}(x,z)|^2) = n_i^2 + \alpha_i \frac{|\mathcal{E}(x,z)|^2}{1 + \mathcal{X}|\mathcal{E}(x,z)|^2} . \qquad (4.3)$$

Note that in the limit $\mathcal{X} = 0$ we get back the previously used Kerr-type nonlinearity, eq. 2.16. The saturation parameter takes care of the fact that the nonlinearity cannot increase indefinitely as the input power goes up.

Figures 4.4(a-d) display the wave emission for four different values of the saturation parameter including the ideal case where $\mathcal{X} = 0$. We used an input beam flux of $S_{in} = 0.6$ which was shown in fig. 2.8(a) to produce three solitons in the ideal case. As $\mathcal{X}$ increases from 0.0 to 0.5 we see a successive decrease in the number of waves emitted. We can explain this by noting that S_c, the critical flux, is an increasing function of $\mathcal{X}$. As we discussed in section II.3.c, wave emission does not occur for $S < S_c$ and now because S_c increases with $\mathcal{X}$, so does the threshold for wave emission. Saturation therefore distorts the dispersion curve causing the local

maximum at S_c to increase.

An important fact to keep in mind is that in the presence of absorption solitons are not emitted, but solitary waves are. We must be careful to replace soliton emission with wave emission in our discussion as we did above. The solitary-wave nature of the emitted waves was established by colliding these waves with copies of themselves. Contrary to the soliton case, the two colliding waves do not simply pass through each other with only a phase shift, but they leave behind a stationary residue. Figure 4.5 shows this collision and the resulting residue. It is not surprising that the waves are not solitons but it is reassuring that waves do continue to be emitted in the presence of saturation.

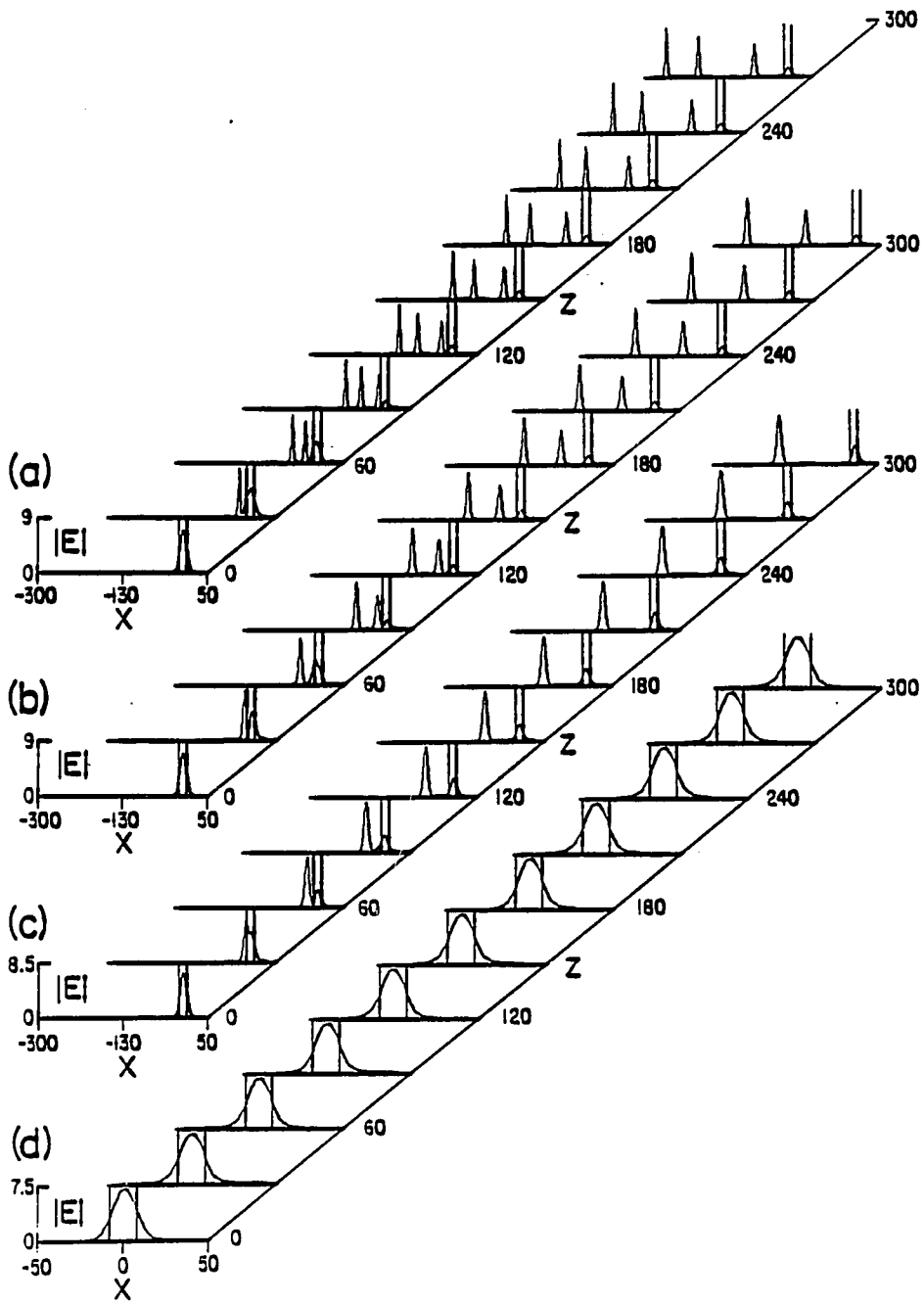

Fig. 4.4. Soliton and solitary-wave emission in the presence of saturation for an input flux S_{in} = 0.6 and (a) $\mathscr{X}$ = 0, (b) $\mathscr{X}$ = 0.02, (c) $\mathscr{X}$ = 0.05, (d) $\mathscr{X}$ = 0.5.

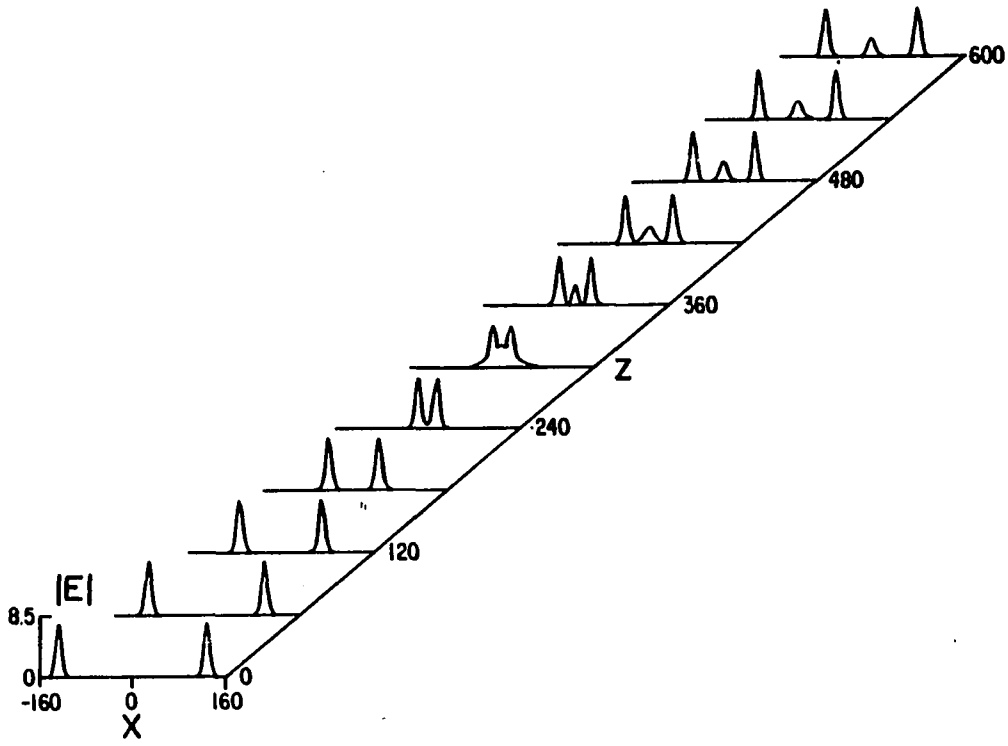

Fig. 4.5. Solitary-wave collision. The solitary-wave component from the final frame in Fig. 4.4(c) has been collided with a copy of itself in the nonlinear medium with the waveguide removed.

IV CONCLUSION

For my thesis I theoretically studied the effects of various complications on the excitation and propagation of nonlinear guided waves. By correctly modeling the complication in the nonlinear wave equation and then using the beam propagation method we studied these effects. We found that the absorptive profile of a nonlinear waveguide has a dramatic effect on the propagation of TE_0 nonlinear guided waves. For stability, it is preferable that the film exhibit lower absorption than the cladding and substrate. Also for successful excitation of branch II nonlinear guided waves the above preference is observed and if the absorption is not too strong results reminiscent of the lossless case can be achieved. Fortunately, this preference is, in general, realized by the choice we have made of nonlinear cladding, because the largest absorption coefficient is that associated with the nonlinear refractive effect.

The effect of various complications on soliton emission was also studied. Linear absorption, input beam misalignments and nonlinear saturation were modeled in the nonlinear wave equation and the beam propagation method was employed to propagate an input Gaussian beam. We found again that for small absorption coefficients results reminiscent of the lossless case do survive although we no longer have a true soliton. For larger absorption coefficients the emitted wave packet dies quickly and for even larger coefficients no packet is emitted. When the input Gaussian beam is drastically misaligned soliton emission still persists although sizable amounts of radiation are produced along with the soliton and guided wave components. In the case of nonlinear saturation we found that solitary waves and not solitons are produced and by increasing the saturation parameter $\mathscr{X}$ we can

decrease the number of solitary waves produced to zero.

Furthermore, we found it encouraging that although the basic phenomena of nonlinear guided waves and soliton emission may change form slightly, in general, they are resilient enough to survive small amounts of those various complications. It should be especially encouraging to those who wish to eventually observe soliton emission in an experimental situation. Also useful is the information obtained on the various limitations of the optical devices, i.e. if we know the largest saturation parameter tolerable we can chose materials with one less than this limit. In conclusion, the most important accomplishment of this theoretical study is the proof that results similar to the lossless case are achieved if the complications are not too large.

LIST OF REFERENCES

1. See, for example, Yariv, Introduction to Optical Electronics (Holt, Rinehart and Winston, New York, 1976, 2nd ed.) p. 354.

2. See, for example, Kogelnick, Topics in Applied Physics Vol. 7, ed. by T. Tamir (Springer-Verlag, New York, 1982, 2nd ed.) p. 13.

3. M. Miyagi and S. Nishida, SCI. REP. RITU, B 24, 53 (1972).

4. N. N. Akhmediev, Sov. Phys. JETP 56, 299 (1982).

5. N. N. Akhmediev, K. O. Boltar and V. M. Eleonskii, Opt. Spectrosc. (USSR) 53, 654 (1983).

6. A. A. Maradudin, "Nonlinear surface electromagnetic waves," in *Proceedings of the Second International School on Condensed Matter Physics*, Varna, Bulgaria, (1983). [Singapore: World Scientific, (1983)].

7. F. Lederer, U. Langbein and H. E. Ponath, Appl. Phys. B 31, 69 (1983).

8. U. Langbein, F. Lederer, H. E. Ponath and U. Trutshel, J. Mol. Struct. 115, 493 (1984).

9. A. D. Boardman and P. Egan, Phil. Trans. Royal Soc. London A 313, 363 (1984).

10. A. D. Boardman and P. Egan, J. Phys. Colloq. C 5, 291 (1984).

11. G. I. Stegeman, C. T. Seaton, J. Chilwell and S. D. Smith, Appl. Phys. Lett. 44, 830 (1984).

12. D. Mihalache and H. Totia, Rev. Roumaine Phys. 29, 365 (1984).

13. U. Langbein, F. Lederer and H. E. Ponath, Optics Comm. 46, 167 (1983).

14. F. Lederer, U. Langbein and H. E. Ponath, Appl. Phys. B 31, 187 (1983).

15. A. E. Kaplan, Sov. Phys. JETP 45, 896 (1977).

16. A. E. Kaplan, JETP Lett. 24, 114 (1976).

17. C. T. Seaton, J. D. Valera, R. L. Shoemaker, G. I. Stegeman, J. T. Chilwell and S. D. Smith, IEEE J. Quant. Electron. 21, 774 (1985).

18. A. D. Boardman and P. Egan, IEEE J. Quant. Electron. 22, 319 (1986).

19. L. Wendler, Phys. Status Solidi B 135, 759 (1986).

20. U. Langbein, F. Lederer, H. E. Ponath, Optics Comm. 53, 417 (1985).

21. U. Langbein, F. Lederer, T. Peshel and H. E. Ponath, Optics Lett. 10, 571 (1985).

22. G. I. Stegeman, C. T. Seaton, J. Ariyasu, T. P. Shen and J. V. Moloney, Optics Comm. 56, 365 (1986).

23. G. I. Stegeman, J. Ariyasu, C. T. Seaton, T. P. Shen and J. V. Moloney, Appl. Phys. Lett. 47, 1254 (1985).

24. C. T. Seaton, X. Mai, G. I. Stegeman and H. G. Winful, Opt. Eng. 24, 593 (1985).

25. J. A. Fleck, J. R. Morris and E. S. Bliss, IEEE J. Quant. Electron. 14, 353 (1978).

26. J. V. Moloney, J. Ariyasu, C. T. Seaton and G. I. Stegeman, Appl. Phys. Lett. 48, 826 (1986).

27. E. M. Wright, G. I. Stegeman, C. T. Stegeman and J. V. Moloney, Appl. Phys. Lett. 49, 435 (1986).

28. N. N. Akhmediev, V. I. Korneev and Y. V. Kuz'menko Sov. Phys. JETP 61, 62 (1985).

29. L. Leine, C. Wachter, U. Langbein and F. Lederer, Opt. Lett. 11, 590 (1986).

30. N. N. Rosanov, Opt. Spektrosk. 47, 606 (1979) [Opt. Spectrosc. (USSR) 47, 335 (1979)].

31. W. J. Tomlinson, J. P. Gordon, P. W. Smith and A. E. Kaplan, Appl. Opt. 21, 2041 (1982).

32. E. M. Wright, G. I. Stegeman, C. T. Seaton, J. V. Moloney and A. D. Boardman, Phys. Rev. A 34, 4442 (1986).

33. See, for example, A. Yariv, Quantum Electronics (Wiley, New York, 1975, 2nd ed.) p. 155.

34. M. Gubbels, E. M. Wright G. I. Stegeman, C. T. Seaton and J. V. Moloney, Opt. Comm. 61, 357 (1987).

35. J. Ariyasu, C. T. Seaton and G. I. Stegeman, Appl. Phys. Lett. 47, 355 (1985).

36. M. A. Gubbels, E. M. Wright, G. I. Stegeman, C. T. Seaton and J. V. Moloney, J. Opt. Soc. Am. B 4, No. 11, 1837 (1987).